The effect of initial pH on surface properties of ferric ion precipitates formed during microbial oxidation of ferrous ion by *Leptospirillum ferriphilum* in a CSTR

By

Bongolwethu Professor Mabusela

Dissertation presented for the Degree of

Master of Engineering degree

In the Department of Chemical Engineering

Cape Peninsula University Of Technology

Supervisor: Prof T.V Ojumu

Cape Town Campus

2017

CPUT Copyright Information

DECLARATION

I, Bongolwethu Professor Mabusela, declare that the contents of this dissertation represent my own unaided work, and that the thesis has not previously been submitted for academic examination towards any qualification. Furthermore, it represents my own opinions and not necessarily those of the Cape Peninsula University of Technology.

……. ……..

Signed Date

ABSTRACT

While bioleaching is a proven technology for the efficient recovery of base metals from sulphide minerals, its sustenance is dependent on the continuous availability of ferric ion, Fe^{3+}, in soluble form, in the bioleach liquor. However, the solubility of ferric ion is low at higher pH that it tends to precipitate, resulting in the formation of ferric ion precipitates. The formation of ferric ion precipitates in bio-hydrometallurgy decreases the leaching efficiency by trapping the leached metals in solution through an adsorption mechanism which is not well understood. Although the surface properties of the precipitate could be linked to its metal adsorption properties, there has not been a detailed study that gives any indication or explanation of the adsorption mechanism. Therefore, the aim of this study was to investigate the effect of initial pH on the surface properties of ferric ion precipitate and relate this to the adsorption characteristics of the precipitate for desired metals.

Biooxidation experiments catalysed by *Leptospirillum ferriphilum* were conducted in a CSTR with a working volume of 1L. The biooxidation experiments were conducted at pH values of 1.3, 1.5, 1.7, 1.9 and 2.2 at a constant temperature of 35 ^{0}C for 14 days. The recovered precipitates were characterized by X-ray diffraction, elemental analyses, SEM, particle size distribution (PSD) and zeta potential. Zeta potential measurements were conducted to investigate what role initial pH plays in modifying the precipitate surface charge and what role the surface charge of each precipitate plays in the nature of adsorption of copper ions onto the precipitate surface. The amount of copper adsorbed onto the precipitate was quantified by the magnitude of the change in surface charge after adsorption experiments.

Quantification results showed that the amount of ferric ions precipitates formed increased from 4.31g to 13.26g with an increase in initial pH (from 1.3 to 2.2). The results also showed that significant precipitation of ferric ion occurred during the exponential phase while insignificant precipitation was observed during the stationary phase.

The XRD patterns indicated that the formed precipitates were a mixture of a well-ordered potassium-hydronium jarosite with minor amounts of goethite on the precipitates formed at pH 1.9 and 2.2. The low background counts indicated that the precipitates were well crystalline and were free of amorphous phases. The SEM analyses showed the precipitates to possess unsmooth surfaces with no sharp edges, except for the precipitates formed at pH 1.9 and 2.2

which showed the development of sharp edges. The PSD results revealed that jarosite-type compounds do not form directly from solution but develop from polymeric intermediaries. The number of particles was found to increase with an increase in pH due to increased amount of precipitate formed.

The zeta potential results showed that the precipitates carried a net positive charge over the experimental pH range studied except for the precipitate formed at pH 2.2 which carried a net negative charge. The magnitude of the positive surface charge of the precipitates was found to decrease with increase initial experimental pH. The amount of copper ions adsorbed onto the precipitate surface increased with increase initial synthesis pH because of the weak electrostatic repulsion forces between the precipitate surface and copper ions. The results illustrated a direct relationship between the amount of copper adsorbed onto the surface and the surface charge of the precipitate. It was concluded that the adsorption of copper onto ferric ion precipitates is highly influenced by the surface charge of the precipitate.

This study revealed that surface charge of a precipitate could give an indication of its metal adsorption capacity. Although the study reveals that in order to increase bioleach efficiency, bioleach liquor conditions should be maintained such that the resulting precipitates have high surface charge to promote electrostatic repulsion, however, in reality, a compromise must be reached by operating the bioleach system at condition(s) that minimize both ferric ion precipitation and metal adsorption.

DEDICATION

This thesis is dedicated to my late grandmother, Nomziwokuthula Mabusela, whose moral support and prayers through my academic journey I cannot undermine; my beloved mother, Weziwe Mabusela and my stepfather, Xolani Ngwane for their financial assistance, endless love, encouragement and moral support that I am extremely grateful for. To my mother, I salute you Oledy for all your sacrifices that have brought me this far. Finally to my sister, Iviwe Mabusela; cousins, Dikeledi Dikhoedi and Mandla Thwayisa, and my niece, Buhle Manyosi, let this be an inspiration to you.

ACKNOWLEDGEMENTS

I wish to thank the following people who made it possible for me to complete this research:

- Glory be to Thixo whom to all things are possible for giving me the strength, wisdom and courage to pursue this degree.
- My supervisor, Prof T.V Ojumu for giving me such an opportunity to explore this field of research. I am tremendously grateful for his words of encouragement when I felt like giving up and his guidance throughout this work. I thank you Prof for having faith in me.
- H. Small and A. Bester for their technical assistance throughout this project.
- My mentor, Dr. Buntu Godongwana for the motivational words he gave me throughout this study.
- Professor Lisa Du Toit from the University of Witwatersrand for inviting me to her institution to perform the zeta potential analyses and for ensuring that my stay in Johannesburg was pleasant.
- Dr. Phogothi Patrick Komane from the University of Johannesburg for unselfishly training me on the zeta sizer equipment
- Miranda Waldron from UCT for SEM experiments
- Dr. Remy Bucher from Ithemba labs for XRD experiments
- Dr. Mario Alberto Macias from Los Andes University (Colombia) for the helpful discussions we had on research gate about the XRD results interpretation.
- All my postgraduate colleagues (past and present) and the Chemical Engineering staff for their support and assistance
- My girlfriend, Zizipho Nyongwana for the endless love and support she gave me and for always been by my side and believing in me.
- Our in-service trainee student, Bhekokwakhe Mabika for assisting in carrying out some of the experiments

The financial assistance of the National Research Foundation towards this research is acknowledged. Opinions expressed in this thesis and the conclusions arrived at, are those of the author, and are not necessarily to be attributed to the National Research Foundation

LIST OF PRESENTATION

Journal Publication

Mabusela, B and Ojumu, T.V. 2017. The effect of initial solution pH on surface properties of ferric ion precipitates formed during biooxidation of ferrous ion by *Leptospirillum ferriphilum*. Solid State Phenomena, Vol. 262, pp. 403 - 407

Oral presentation

Mabusela, B.P and Ojumu, T.V. 2017. The effect of initial solution pH on surface properties of ferric iron precipitates formed during biooxidation of ferrous iron by *Leptospirillum ferriphilum*. 22nd International Biohydrometallurgy Symposium, TU Bergakademie Freiberg, Germany. 24 – 27 September 2017. (Accepted)

TABLE OF CONTENTS

LIST OF FIGURES

LIST OF TABLES

Chapter 1

INTRODUCTION

1.1 Background

Hydrometallurgy and pyrometallurgy are conventional processes that have been used in the extraction of valuable metals (high-grade ore) such as copper, iron, and gold. In these conventional processes, the sulphide minerals undergo smelting and roasting, which results in emissions of sulphur dioxide which is of environmental concern. This requires the application of emission control systems which increases the capital and operating costs of these processes (Kazadi, 2007). Due to the increase in demand for minerals and depletion of high-grade ores, conventional processes are becoming less of interest. These processes have proven to be uneconomical, complex in operation and environmentally unfriendly (Vossoughi et al., 2007). Alternative techniques that offer economic, environmental and technical advantages over conventional techniques have been under development. Biohydrometallurgy has emerged as an alternative technology for the extraction of low-grade ores, especially copper and gold, due to its operational complexity and environmental advantages (Gahan et al., 2012). Several studies have explored different aspects of biohydrometallurgy with a view to optimize the process such that it reaches a stage where it can oust conventional processes

Bioleaching is the extraction of valuable metals from their ores which is facilitated through the use of living organisms (Devisia and Nataraja, 2004). The process involves the solubilisation of one or more components of a complex solid into a liquid phase. Bioleaching has been applied in the pre-treatment of gold ores prior to cyanidation and in the extraction of copper from copper sulphide ores. There is also considerable potential for bioleaching and pretreatment of a wide range of base metals and platinum group metals, moreover, the process is presently under development for the extraction of minerals such as cobalt, uranium and zinc from their ore deposits (Kazadi, 2007, Ojumu, 2008).

Although various bioleaching techniques have been developed for mineral extraction, however, the selection of technique is dependent on the scale of operation, the grade of the ore being processed and its suitability for prior milling and concentration (Archer, 1997, Ojumu, 2008). Despite Heap bioleaching being an established technology for the extraction of copper from low-

grade copper sulphide ores, it is limited in its control over the prevailing operating conditions. Moreover, parameters such as temperature and pH may vary widely, temporarily and spatially within the heap (Chowdhury, 2014). On the other hand, tank bioleaching has made a lot of progress, as it achieves 95 to 98% metal recovery after 5 days and it also offers good control of operating conditions, allowing it to be operated mostly under optimum conditions (Ojumu, 2008, Kazadi, 2007).

Microbial ferrous ion oxidation is a critical sub process of bioleaching and has been regarded as the main driving force of bioleaching (Wanjiya, 2013). The main role of microorganism in the dissolution of sulphide minerals is based on the bacterial oxidation of ferrous ion (Fe^{2+}) to ferric ion (Fe^{3+}). Ferric ion plays a vital role as a critical reagent for the oxidation of many sulphide minerals of industrial relevance. Ferric ion in solution leaches sulphide minerals, releasing the metal of value into solution and sulphur species, while it's reduced back to ferrous ion.

Oxidation of ferrous ion in the bioleaching process causes the formation of different types of iron precipitates (Nazari et al., 2014). In many processes, these precipitates represent the exit route for undesired iron from the circuit (Kaksonen et al., 2014b). In conventional hydrometallurgical flow sheets precipitation occurs under controlled conditions to yield relatively well defined compounds such as hematite, goethite or crystalline jarosite (Gramp et al., 2008), while in less controlled conditions, especially in bioleaching and general heap leaching, a poorly defined mixture of various forms of iron precipitates occurs, containing ferric hydroxides, oxyhydroxides, schwertmannite and jarosites etc. (Gramp et al., 2008, Rodger and Herbert, 1997). The precipitation of ferric ion is orders of magnitude higher in biological systems as compared to chemical and abiotic systems (Lazaroff et al., 1982, Sasaki and Konno, 2000).

1.2 Background to research problem and motivation

During bioleaching of sulphide minerals, ferrous ion (Fe^{2+}) is oxidized to ferric ion (Fe^{3+}) which acts as a strong leaching reagent for the dissolution of most sulphide minerals. Ferric ion, however, has a very low solubility at pH > 2.2 (Wanjiya, 2013, Grishin et al., 1988b) that creates a tendency to precipitate, promoting the formation of various types of iron precipitates. These precipitates are amorphous and have high surface area due to their colloidal nature and may tend to adsorb significant amounts of valuable metals thus preventing their release into solution (Nheta and Makhatha, 2013), Also, this may interfere with kinetics process of microbial

oxidation of ferrous ion (Liu et al., 2017). In addition to the effect they have on the concentration quantities of ions that are required for nutrients for microbial growth (Nazari et al., 2014), ferric ion precipitates also prevent bacteria and soluble ferric-ion from accessing the mineral sulphide surface (Córdoba et al., 2008a, Watling et al., 2009, Pina et al., 2005). Most importantly, ferric ion precipitates are known to reduce extraction efficiency of bioleach by trapping valuable metals by an adsorption mechanism that is not well documented. This has been confirmed in studies such as Nheta and Makhatha (2013), where treatment of jarosite released significant amounts of Ni from a preceding bioleaching process as well as Ju et al. (2011) who recovered significant amounts of zinc, silver, lead, copper and cadmium from jarosite residue produced during zinc hydrometallurgy.

Characterization studies of ferric ion precipitates have been reported extensively but these studies only extend up to mineralogy, physical and chemical composition (Kaksonen et al., 2014b, Chiranjit, 2013, Grishin et al., 1988b, Bigham et al., 2010, Nazari et al., 2014, Wang et al., 2006b, Lazaroff et al., 1982, Pham et al., 2006, Toro et al., 1988, Liu et al., 2009). Moreover, Gasharova et al. (2005) emphasized that a detailed characterization of ferric ion precipitates with respect to the above properties was crucial to understanding the mechanisms and kinetics of the reactions of ferric ion precipitates in aqueous solutions. The recent simulation study conducted by Hudson-Edwards and Wright(2011) proved that the incorporation of impurities on particles was influenced by the surface structure of the particles. This information provided a motivation to understand the interactions of ferric ion precipitates with process kinetics and adsorption of valuable metals(Hudson-Edwards and Wright, 2011). Although there could be varieties of ferric ion precipitates in a typical bioleach process (Gramp et al., 2008, Rodger and Herbert, 1997), it is still not known whether the adsorption action is due to a specific type of ferric precipitate. Therefore, an investigation on surface properties of these precipitates is important, especially if a link can be established between surface properties and leach solution conditions, and the adsorption characteristics of the precipitates for desired metals.

This study attempts to provide an understanding of the effect of changing solution condition with respect to solution pH on surface property of ferric ion precipitates and to relate this to the adsorption characteristic of the respective precipitates for desired ion (for example copper ions). This knowledge will provide a fundamental understanding of the surface properties of precipitates and an indication of how to manipulate solution pH to modify surface charge of precipitates as well as provide a strategy of operation/design of bioleach and ferrous

biooxidation processes that minimize the loss of base metals. The results of this study would minimize the adsorption of base metals onto precipitates and may eliminate the necessity to further treat the precipitate with the view to recovering these metals, which subsequently results in minimized operational cost.

1.3 The research objectives

The overall objective of this study is to investigate the effects of solution pH on the quantification and surface properties of ferric ion precipitates which are formed during microbial ferrous ion oxidation. This is to provide a fundamental understanding of the relationship between operating solution pH and surface properties of ferric ion precipitates and relate surface charge of precipitates to its adsorption characteristics. In more specific terms the objectives of this study are as follows:

- To investigate ferric ion precipitate formed during biooxidation with a view to understanding the effect of initial pH on the type of precipitate formed.
- To investigate the effect of changing solution pH on the surface properties of ferric precipitate formed with a view to establishing a relationship link between solution pH and surface properties of the formed precipitates.
- To investigate whether a relationship exists between the surface properties of precipitates and adsorption characteristics for valuable metals.

1.4 Research hypothesis and questions

The hypothesis formulated and the questions derived in this study are as follows:

Hypothesis 1: The quantity of ferric precipitate is affected by many factors, of which the least studied are reactor configuration and type of strain used. In bioleaching, microorganisms act as a biocatalyst. It is believed that each type of strain will have different effect on the quantity of precipitate formed depending on how effective the strain is in the prevailing conditions.

- How does reactor configuration and type of strain affect the quantity of ferric ion precipitate formed and how does this amount compare to values in literature?

Hypothesis 2: During biooxidation of ferrous ion mediated by *Leptopsirillum ferriphilum*, ferric ion precipitates are formed. Changes in solution conditions, especially pH, will result in altering the surface charge of the respective ferric ion precipitates.

- How do changes in solution pH affect the surface charge of ferric ion precipitates and how does this directly affect the adsorption characteristics of the precipitates for the metal?

Hypothesis 3: The type of ferric ion precipitate formed during biooxidation is depended on solution conditions and concentrations in the medium but because potassium jarosite has higher preference compared to other precipitates, the ferric ion precipitate produced in the targeted solution pHs will merely be potassium jarosite with possibly some minor amounts of extra phases at higher pH.

- How do changes in solution pH affect the type of ferric ion precipitate formed?

Hypothesis 4: In batch experiments of *Leptospirillum ferriphilum,* ferrous ion is oxidized to ferric ion. Precipitation of ferric ion begins as early as when the microbes are in the lag phase. It is also hypothesized that jarosite-type compounds are not likely to be the primary products in biooxidation systems.

- What is the initial stage for ferric ion precipitation and do jarositic type compounds form directly without precursor species?

1.5 Significance of the study

The main purpose of this study is to provide an understanding of the relationship between operating conditions and surface properties (mainly surface charge) of the ferric ion precipitates formed during microbial oxidation of ferrous ion by *Leptospirillum ferriphilum.* This is to understand the adsorption characteristics of ferric ion precipitates for valuable metals, which will subsequently assist in the improvement of producing ferric ion precipitates with controlled kinetics, as well as modified surface properties that will promote minimum adsorption of valuable metals. This will increase their recovery while maintaining higher biooxidation rates.

The results will also serve to provide a database for the quantification of iron precipitates in a typical bioreactor system and may provide a guide in the design of full industrial scale bioreactors. The overall significance of this study is to improve the extraction efficiency of valuable metals as well as to maintain sustainability in biohydrometallurgical operations. The

knowledge gained from this work would be of value on a global scale, specially for countries that use bioleaching/biooxidation as the key technology for metal extraction.

1.6 Thesis outline

This thesis is divided into seven chapters; the first chapter introduces the thesis through a brief summary of the research background, the research problem, the significance of the research and the questions the research seeks to answer.

The second chapter includes a detailed critique of relevant literature that exist. While chapter three includes details of the reactor set-up as well as the operation and analytical methods utilized. Furthermore, it discusses the experimental approach of the study and gives a description of the material as well as the bacterial culture and growth medium employed.

In Chapters four and five, the experimental results and discussions of these results are presented. Chapter four specifically discusses the effect of changes in solution pH on the kinetics of ferric ion precipitation and quantification, while chapter five is focused on the surface properties and characteristics of the precipitates.

Chapter 6 is the concluding chapter of the thesis and it includes a summary of the study and recommendations for future work, while chapter seven is a list of reference of the sources consulted in this study.

Chapter 2

Literature review

2.1 Bioleaching

2.1.1 Historical background

Bioleaching has been in practice since the ancient times, although the principles governing it were unknown then (Kazadi, 2007). The Chinese are believed to have been the first to practice the form of bioleaching as far back as 100 – 200 BC and probably even before any other nation. They implemented this technology for the production of copper on a commercial scale with a process thought to be developed by medieval Chinese alchemist (Lung, 1986). Despite the long-standing practice of leaching of metals from sulphide minerals, the role of microorganisms in this process was only discovered in the mid-twentieth century (Rawlings, 2002, Lung, 1986).

According to Ehrlich (2001), the reason for this belated discovery was that the existence of bacteria, in general, was not known until the middle of the seventeenth century. It is believed that the microbes played a role in even earlier activities at the Rio Tinto mine in Spain by the 18^{th} century (Rawlings, 2002). Pre-Romans recovered silver and the Romans recovered copper from a deposit located in the Seville province in the South of Spain, which later became known as the Rio Tinto mine. The Rio Tinto (Red sea) obtained its name from the red color imparted to the water by the high concentration of ferric ion (Rawlings, 2002). For many years this technique seemed to work only at the Rio Tinto mine and not anywhere else due to the Rio Tinto ore or the Spanish climate which had an obscure and mysterious quality. South-western states of the U.S.A attempted leaching of low-grade ore but did not succeed (Rossi, 1990).

However, modern bioleaching only began when Temple and Colmer (1951) isolated and described *Acidithiobacillus ferrooxidans* to be one of the organisms responsible for acid mine drainage. Thereafter, Intensive research began after Bryner et al. (1954) and Bryner and Anderson (1957) provided evidence of the ability of *At. Ferrooxidans* to oxidise other metal sulphides. The researchers proved that the production of soluble iron, copper and sulphiric acid in the leaching water was not due to simple chemical processes but were a result of the action of microorganisms. The ability of *At.Ferrooxidans* to solubilise metal sulphides was further elaborated by Duncan et al. (1967), where they published a list of nineteen metal sulphides

which were solubilised by *At. Ferrooxidans*. The microorganism gained attention and has since then been isolated from all the acid drainage waters flowing from ore-bodies, mines and dumps of low-grade ore. Thus a correlation was established between the presence of bacterium and the dissolution of metals in copper leaching operations (Brierley, 1982).

The Kennecott Copper Company, in the 1950s, was the first to successfully use the process of commercial application of biohydrometallurgy to extract copper from submarginal-grade and run-of-mine materials, using a technique known as dump leaching (Olson et al., 2003, Acevedo, 2000, Brierley and Brierley, 2001). On the other hand, commercial heap leaching became operational in the 1960s since the design of dump leaching did not promote microbial growth and activity of microorganism due to poor aeration (Rossi, 1990). Therefore, heaps were specifically designed to provide good aeration and other parameters to ensure high activity of the bacteria and hence better recovery for metals (Olson et al., 2003, Rawlings et al., 2003).

Copper leaching from heaps was initiated in the mid-1980s and since then a growing increase in copper heap bioleaching operations have been in progress i.e. Fairview operation in South Africa (Brierley and Brierley, 2001). The first copper mine which was commissioned during the mid-1980s in Munera Pudahuel in Chile switched from mixed acid and bacterial leaching to full heap bioleaching of an ore containing 1 to 2 % copper with a production of 14000 tonnes of fine copper per year. Since the 1980s, bioleaching has developed significantly (Brierley and Brierley, 2001, Deveci et al., 2004).

Although early commercial applications of bioleach technology processed submarginal grade copper-bearing rock in dumps, however, recent applications of the technology use engineered bioleach heaps. It is noteworthy that all of these operations are in countries of the Southern Hemisphere. Moreover, the pioneering work in North America was not advanced to commercial application. In total, Eleven copper bio heap leach plants and one in situ bioleach operation have been commissioned since1980 (Table 2.1)(Brierley, 1997).

Table 2.1: Commercial copper bio heap leach plants

Operation	Reserves (Mt)	Ore processed	Copper production (t/a)	Copper grade (%)
Toquepala & Cuajone, Peru	134.3	128500	40000	0.24
S&K Copper, Myanmar	435	30000	39000	0.29
Lomas Bayas, Chile	72.7	124000	75000	0.31
Zijinshan Copper Mine, China	400	8400	10000	0.43
Lisbon Valley, Utah, USA	40.4	18300	27000	0.46
Cerro Verde, Peru	1000	63000	100000	0.51
Morenci, Arizona, USA	3450	88000	110000	0.52
Escondida Norte, Chile	1701	110000	180000	0.55
Skouriotissa (Phoenix pit), Cyprus	15	3000	5200	0.57
Andacollo, Chile	32	15000	20500	0.80
Zaldivar, Chile	235	54500	150000	0.91
Dos Amigos, Chile	5	3000	10000	1

Source: (Neale et al., 2011)

Currently, bacterial leaching of copper, cobalt and biooxidation of refractory gold concentrates are well established large-scale processes that are carried out with the use of heap and tank reactors. According to Brierley and Brierley (2001), seven plants have been commissioned for biooxidation pretreatment of sulfidic-refractory gold concentrates which employ large, aerated, stirred-tank reactors for the biooxidation of pyrite and arsenopyrite minerals locking the gold values. The first commercial plant for bioleaching and recovery of cobalt has been commissioned in Uganda for treating cobaltiferous pyrite concentrate, grading 1.38% cobalt with 92% cobalt recovery (Brierley and Brierley, 2001). Even though heap operation is simple and adequate to handle large volumes of minerals, their productivity and yields are limited because of the severe difficulties in exerting an adequate process control (Acevedo, 2000).

Recently, extensive attention has been paid to understanding the governing mechanisms and principles of heap bioleaching (Petersen and Dixon, 2006, Petersen and Dixon, 2007, Casas et al., 1998) so as to make the operation of heap bioleaching more efficient and effective.

2.1.2 The mechanism of bioleaching

Acidithiobacillus ferrooxidans was considered to be the principle microorganism responsible for bioleaching of mineral sulphides (Lundgren and Silver, 1980). Silverman and Ehrlich (1964) studied the oxidation of pyrite (FeS_2) and were the first to propose the two mechanisms by which microorganisms (*Acidithiobacillus ferrooxidans*) catalyze the dissolution of metal sulphides.

2.1.2.1 The indirect leaching mechanism

The first mechanism was referred to as 'indirect leaching' (Figure2.1). This mechanism described the critical importance of ferric ion as an oxidant in the process of mineral sulphide oxidation. Ferric sulphate was believed to originate from pyrite oxidation in aerated water under the following reactions:

$$FeS_2 + 3.5O_2 + H_2O \rightarrow FeSO_{4(aq)} + H_2SO_{4(aq)} \quad 2.1$$

$$4FeSO_{4(aq)} + 2H_2SO_{4(aq)} + O_2 \rightarrow 2Fe_2(SO_4)_{3(aq)} + 2H_2O \quad 2.2$$

Reaction 2.2 proceeds rapidly in the presence of iron-oxidising bacteria i.e*. Acidithiobacillus ferrooxidans* in this case. The ferric ion in solution oxidizes the metal sulphide to corresponding sulphides and elemental sulphur, solubilizing the metal of interest:

$$MS + 2Fe^{3+} \rightarrow 2Fe^{2+} + S^0 + M^{2+} \quad 2.3$$

The ferric ion, in turn, is reduced back to ferrous ion. The role of bacteria is to promote continuous leaching of the mineral sulphide by catalyzing the cyclic regeneration of ferrous to ferric. According to Suzuki (2001), the classical understanding of indirect pyrite leaching before 1980 was generally accepted to proceed according to the following reactions:

$$FeS_2 + 2Fe^{3+} \rightarrow 3Fe^{2+} + 2S^0 \downarrow \quad \text{(Chemical oxidation with ferric ion)} \quad 2.4$$

$$2Fe^{2+} + \frac{1}{2}O_2 + 2H^+ \xrightarrow{iron-oxidising\ bacteria} 2Fe^{3+} + H_2O \text{(Bacterial mediated ferrous oxidation)} \quad 2.5$$

$$S + \frac{3}{2}O_2 + H_2O \xrightarrow{sulphur-oxidising\ bacteria} H_2SO_4 \text{(Bacterial mediated sulphur oxidation)} \quad 2.6$$

.

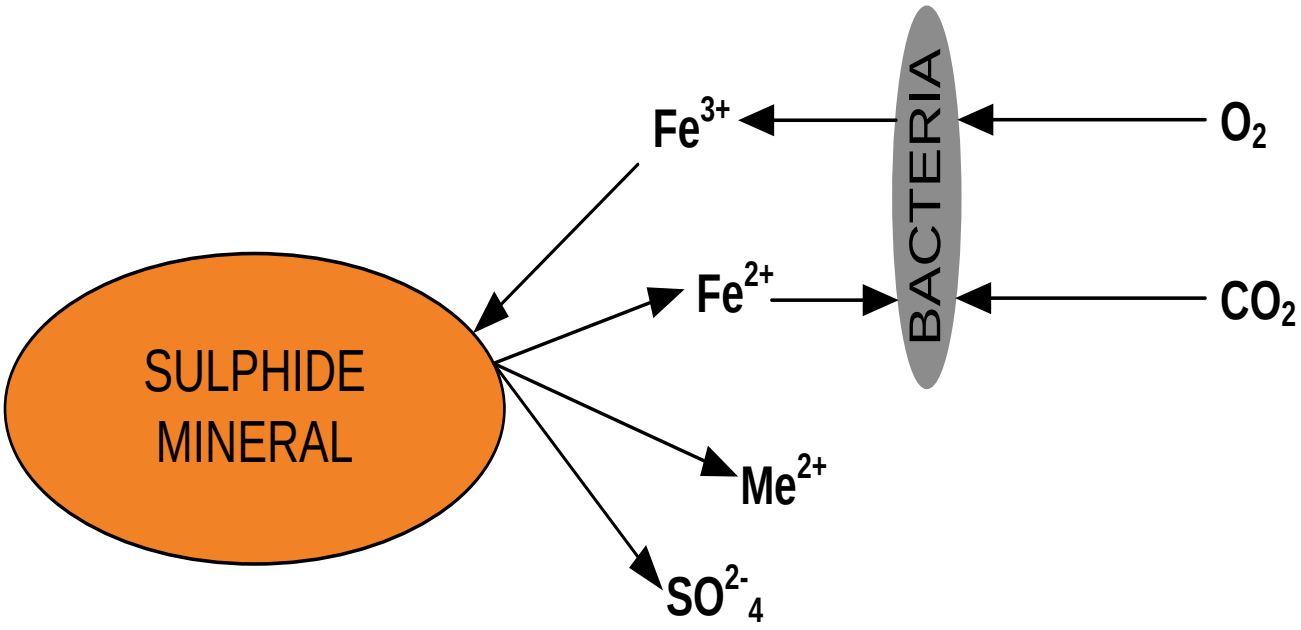

Figure2.1: Indirect bacterial oxidation of sulphide mineral modified from Boon (1996)

2.1.2.2 The direct mechanism

The second leaching mechanism proposed by Silverman and Ehrlich (1964), which is currently globally debated, was described as the direct mechanism (Figure 2.2). In this mechanism, the attack is believed to proceed by the enzymatic attack, whereby the organism engages in intimacy with the sulphide mineral's surface according to reaction 2.7.

$$MS + 2O_2 \rightarrow M^{2+}{}_{(aq)} + SO_4^{2-} \qquad 2.7$$

In this mechanism, it is assumed that the bacteria associates closely with the sulphide mineral surface and that the sulphur moiety of the mineral sulphide is biologically oxidized (Suzuki, 2001). However, the specific mechanism by which this occurs has not yet been elucidated (Boon, 1996). Bennett and Tributsch (1978), provided evidence for the direct leaching mechanism from scanning electron microscopy (SEM) which revealed bacterial etching pits in characteristic patterns.

However, it is still not clear if a direct or indirect mechanism applies in a particular biooxidation process. Boon (1996) discusses methods that have been used in literature to discriminate between the direct and indirect mechanism.

.

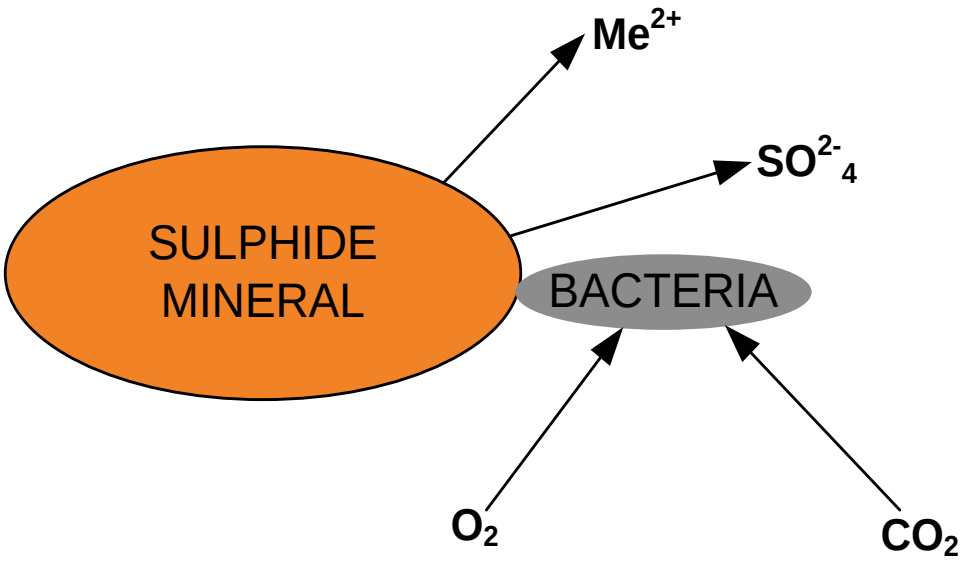

Figure 2.2: Direct mechanism of sulphide minerals (Boon, 1996)

2.1.2.3 Thiosulphate and polysulphide mechanism

Bacterial leaching of metal sulphides occurs through two indirect mechanisms, firstly, by thiosulphate and secondly through polysufides (Schippers and Sand, 1999).

Schippers et al. (1996), proposed a leaching mechanism which focused on intermediate sulphur species that were formed during oxidation of pyrite by *Leptospirillum ferrooxidans* and *Acidithiobacillus ferrooxidans*. The researchers discussed the polysulphide mechanism on pyrite leaching mediated by ferric ion. The thiosulphate mechanism was dependent on the oxidative attack by ferric ion on the acid-insoluble metal sulphides (i.e. pyrite (FeS_2 and molybdenite (MoS_2)) with thiosulfate being the main intermediate and sulphate the end product (Figure2.3). In the polysulphide mechanism, solubilisation of the acid-soluble metal sulphide is initiated through proton (H^+) attack and ferric ion with elemental sulphur being the main intermediate. This elemental sulphur is relatively stable but can be oxidized to sulphate by sulfur-oxidizing microbes (Rawlings et al., 2003).

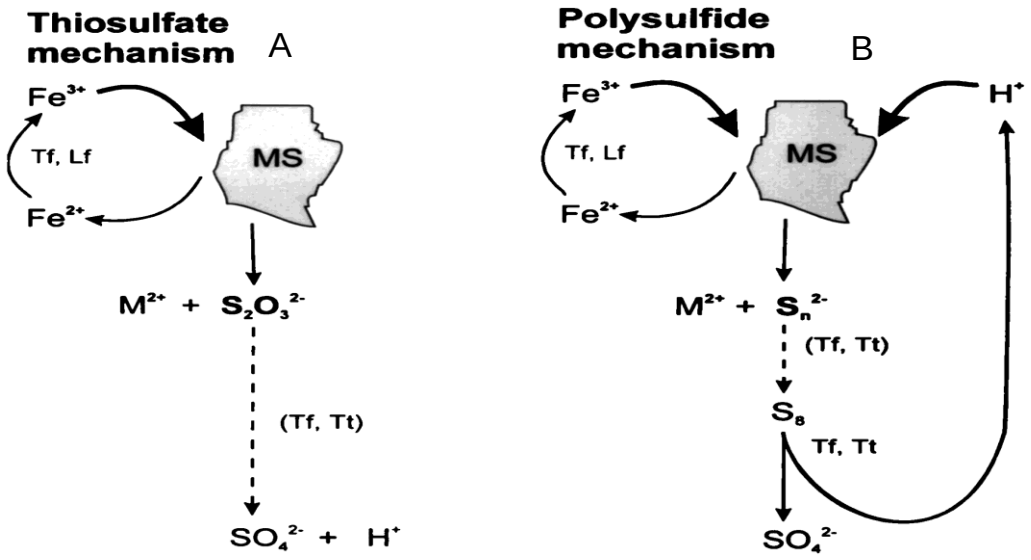

Figure2.3: Schematic representation of bioleaching mechanism showing the sulphur pathways: the thiosulphate pathway (A) and polysulfide pathway (B) (Schippers and Sand, 1999)

2.2 The microorganisms involved in bioleaching

Microorganisms that are involved in bioleaching derive their energy for reproduction and maintenance by oxidizing ferrous ion (Fe^{3+}) and elemental sulphur S^0 (Rawlings, 2002). The microorganisms which are found in bioleaching can be classified into three types: iron-oxidizer, sulphur oxidizers and the heterotrophs. The types of microbes found in both heaps or dump leaching processes are similar to those found in stirred-tank processes, with *At.ferrooxidans, At. thiooxidans* and *L. ferrooxidans* being most frequently detected (Rawlings et al., 2003, Chowdhury, 2014). The diversity of microorganisms is much greater in heap leaching due to the different parameters that exist within it such as; temperature, pH, mineral type, availability of nutrients and biofilm formation (Ojumu, 2008). However, the type of microbes present depends on the properties of the mineral and the prevailing conditions under which the processes are operated (Rawlings, 2005). Most of the widely used microorganisms that have been extensively used in the bioleaching of sulphide minerals with their optimum conditions are given in Table 2.2.

Table 2.2: Characteristics of the most used microbes in bioleaching (Ojumu, 2008)

Microbes	Classification	Oxidation	Temperature (C^0)	pH
Acidithiobacillus ferrooxidans	M	Iron, sulphur	15 – 35 31*	1.4 – 6.0 1.8 – 2.0
Acidithiobacillus thiooxidans	M	Sulphur	10 – 37 28 – 30*	0.5 – 6.0 2.0 – 3.5*
Leptospirillum ferrooxidans	M	Iron	<10 – 45 30 – 37*	1.1 – 4.0 1.6 – 2.0*
Leptospirillum ferriphilum	M	Iron	<45 30 – 37*	1.4 – 1.8*
Acidithiobacilluscaldus	MT	Sulphur	<52 45*	
Acidmicrobiumferrooxidans	MT	Iron	45 – 50*	2*
Leptospirillum thermoferrooxidans	MT	Iron	30 – 55 45 – 50*	>1.3 1.7 – 1.9*
Sulfobacillus acidophilus	MT	Iron, sulphur	30 – 55 45 – 50*	2*
Sulfobacillus thermosulfidooxidans	MT	Iron, sulphur	30 – 60 45 – 48*	1.5 – 5.5 2*
Ferroplasmaacidiphilum	M	Iron	15 – 45 35*	1.2 – 2.2 1.7*
Sulfolobusmetallicus	T	Iron, sulphur	50 – 75 65*	1 – 4.5 1.3 – 1.7*
Metallosphaerasedula	T	Iron, sulphur	50 – 80 75*	1.0 – 4.5 2 – 3*
Acidianusbrierleyi	T	Iron, sulphur	45 – 75 70*	1 – 6 1.5 – 2.0*

M(mesophiles), MT (moderate thermophiles), T(thermophiles)

*(optimum parameters). **Source:** Adapted from Rawlings (2002) and Kinnunen (2004).

These microorganisms can be divided into three distinct groups depending on their tolerance to temperature (Kazadi, 2007):

- Mesophilic bacteria that reproduce at about 10 – 40^{0}C

These are the most important iron-oxidizing microorganisms found in commercial bioleaching systems which operate at temperatures between ambient to 40^{0}C. Mesophilic bacteria are considered to be a consortium of Gram-negative bacteria. Microbes of this group include *Acidithiobacillus ferrooxidans* which are both iron and sulphur oxidizing microbes, the sulphur oxidizing microbes *At.thiooxidans, At. caldus* and the iron-oxidizing *L. ferriphilum* (Ojumu, 2008, Coram and Rawlings, 2002, Watling, 2006)

- Moderately thermophilic bacteria that live at about 40 – 60^{0}C

Moderately thermophilic bacteria are classified as members of the new genus *Sulfobacillus*, while others are still known by their code names (Kazadi, 2007). These microorganisms thrive at temperatures between 40^{0}C and 60^{0}C. *Sulfobacillus* are gram-positive bacteria and endospore-forming bacteria that have been isolated from heaps of mineral waste and biomining operations. They are capable of growing autotrophically and heterotrophically. These microorganisms, when growing autotrophically, feed on ferrous ion, reduced inorganic sulfur compounds and or sulfide minerals as an electron donor. However, they have poor ability to fix CO_2 (Rawlings, 2002)

- Extremely thermophilic archaea that reproduce at 60 – 90^{0}C

According to Rawlings (2005), there are limited reports on types of microbes that occur in mineral treatment processes that operate at temperatures > 70^{0}C than at lower temperatures. Moreover, he noted that such consortia are dominated by archaea rather than bacteria. Archaea have been found to grow at high temperatures such as 90^{0}C feeding on reduced sulfur and at low temperatures. They have been reported to belong to the genus *Acidianus* such as *A.dinfernus.* However, their contribution to industrial bioleaching is still not yet well-established (Rawlings, 2005)

2.2.3 General characteristics of microorganisms

The most important microbes that participate in bioleaching are those that are capable of producing the ferric ion and sulphiric acid required for the leaching reactions. These include the iron- and sulfur-oxidizing chemolithrophic bacteria and archaea. These microbes have similar features that make them suitable for their role in mineral solubilization irrespective of the type of process or temperature at which they are operated. According to Rawlings (2005), four of the most important characteristics of these microbes are**:**

- They grow autotrophically by fixing CO_2 from the atmosphere
- They derive their energy by either oxidizing ferrous ion or reduced inorganic sulfur compounds (some use both) as an electron donor and generally use oxygen as electron acceptor
- They are acidophiles and grow in low pH environments (pH 1.4 – 1.6)
- They are remarkably tolerant of a wide range of metal ions. This characteristic varies within and beyond species.

2.3 The application of bioleaching techniques

Over the years, bioleaching has been proven to be the most reliable technique for processing low-grade concentrates, this is because the use of bioleaching for the production of metals significantly reduces the capital and production costs. Also, it increases the mineral reserves, as the low-grade ores and refractory gold-bearing sulphides, which are now becoming more predominant, can be economically processed (Kazadi, 2007). Even though bioleaching offers better environmental conditions as there are no toxic gas emissions such as sulphur dioxide or arsenic trioxide associated with it, some conventional techniques are preferable over bioleaching for processing of concentrates (Brierley, 2014, Dreisinger, 2006).

The efficiency of the process of bioleaching and biooxidation is controlled by the characteristic of the metal sulphide and for this reason, different techniques are industrially used depending on the grade or value of the ore to be processed. Heaps and stirred tanks are two different engineering applications that are mostly applied and implemented in bioleaching and biooxidation of metal sulphides (Tao and Dongwei, 2014, Kazadi, 2007).

2.3.1 Tank bioleaching

Tank bioleaching is achieved in highly engineered, aerated and continuously stirred tank reactors that are placed in series (Fig. 2.4)(Kazadi, 2007, Rawlings, 2005). The tanks are equipped with agitators that maintain the finely ground sulphide mineral concentrate in suspension and ensure that oxygen is efficiently transferred to the microorganisms (Kazadi, 2007).

Tank leaching involves the processing of mineral concentrates in large bioreactors, and affords more control than irrigation-based operations, therefore, it allows superior leaching efficiencies in terms of rates and metal recovery. Also, microbial activity in stirred-tank reactors can be optimized by adjusting aeration, temperature and pH. In tank bioleaching, stirred-tank reactors are usually arranged in series, with a continuous flow of material into the first, which overflows to the next, and so on until sulphide mineral is oxidized (Brierley, 2014, Gahan et al., 2012). Finely ground mineral concentrate or ore and inorganic nutrients in the form of ammonia and phosphate-containing fertilizers are added to the first tank. The stirred suspension flows through a series of pH and temperature-controlled aeration tanks in which the mineral decomposition takes place (Rawlings et al., 2003), then a large volume of air is blown through each tank, while large agitators ensure smooth suspension of solids (Rawlings, 2002).

One of the strengths of the stirred tank reactors is that mineral solubilization takes days in stirred-tanks reactors compared to the weeks or months it takes in heap reactors (Rawlings, 2005). Also, retention time in the tanks is set to allow sufficiently complete microbial oxidation of the desired minerals. However, there are major constraints on the operation of stirred-tank reactors, in that the quantity of solids which can be maintained in suspension can never exceed 20% pulp density (Rawlings et al., 2003). When compared to other forms of processing techniques, stirred-tank reactors offer an effective level of processing, even though it is not necessarily the most economical (Gahan et al., 2012). Consequently, tank leaching is suitable for concentrates only, since low-grade ores which cannot be economically concentrated cannot cover the processing cost (Kazadi, 2007). Another limitation of the stirred tank reactor is that they are expensive to construct and operate therefore restricting their application to high-value ores and concentrates (Rawlings, 2002).

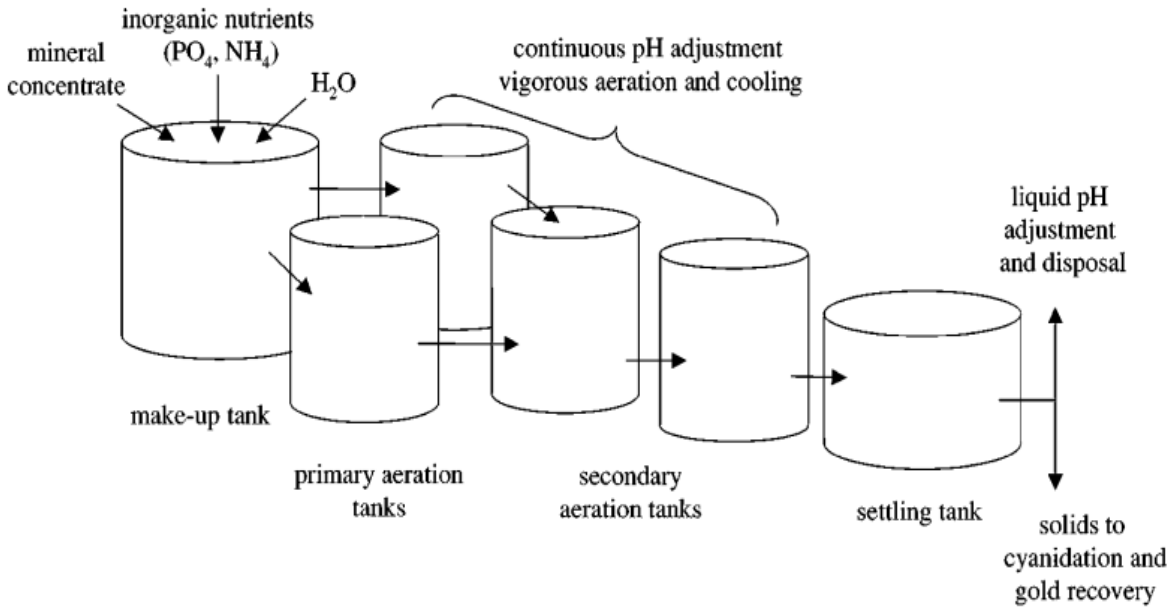

Figure 2.4: Tank bioleaching process (Rawlings, 2002)

The application of stirred-tank bioreactors is mostly applied in commercial operations as a pretreatment process for the recovery of gold from recalcitrant arsenopyrite concentrates (Rawlings et al., 2003). Other researchers (Olson et al., 2003) have noted its potential in the application for recovering nickel, zinc and other metals. Table 2.3 lists commercial mineral bioleaching processes which use stirred-tank bioreactors for pretreatment of refractory gold concentrates.

Table 2.3: Practice of tank bioleaching for pretreatment of refractory gold concentrates

Country	Plant	Design capacity (tons) /day	Operating years	Leaching method
South Africa	Fairview	62	1986 – present	Goldfield's BIOX®
Brazil	Sao Bento	150	1991– 2008	Goldfield's BIOX®
Western Australia	Harbour lights	40	191 –1994	Goldfield's BIOX®
Western Australia	Wiluna	158	1993 –2007	Goldfield's BIOX®
Ghana	Ashanti	960	1994 – present	Goldfield's BIOX®
Western Australia	Youanmi	120	1996 – 1998	BacTechBacox
Peru	Tamboraque	60	1998 – 2003	Goldfield's BIOX®
Australia	Beaconsfield	~70	2000 – 2012	BacTechBacox
China	Laizhou	~100	2001 – present	BachTechBacox
Kazakhstan	Suzdal	196	2005 – present	Goldfield's BIOX®
Australia	Fosterville	211	2005 – present	Goldfield's BIOX®
Ghana	Bogoso	750	2006 – present	BacTechBacox
China	Jinfeng	790	2006 – present	Goldfield's BIOX®
Uzbekistan	Kokpatas	1,069	2008 – present	Goldfield's BIOX®
Peru	Coricancha	60	1998 – 2008	Goldfield's BIOX®

For detail review see (Brierley, 2008)

Source: (Gahan et al., 2012)

2.3.2 Heap and dump bioleaching

Dump and heap leaching are generic processes whereby either run-off mine (dump) or crushed and agglomerated (heap) ore is typically placed either by dumping or stacking at heights ranging from 4 to 10 m for heap leaching and of 19 or higher for dump leaching. Dumps consist of run-off mines which may be piled 350m high. The dumps are subjected to cycles of preconditioning, irrigation, rest, conditioning, and washing, each of which may last for a year (Rawlings, 2002). The process includes applying acidified water to the top surface of the dump using sprinklers or drippers. As the solution percolates through the dump, favorable conditions develop for the growth of naturally-occurring microorganism which catalyzes the oxidation of the copper sulfide minerals. The copper is dissolved in the leach solution and percolates to the base

of the dump where the pregnant leach solution (PLS) is collected and passed to a solvent extraction/electrowinning process for the production of copper cathodes. Then, raffinate from the solvent extraction circuit is recycled to the top of the dump. However, leaching of copper is measured in decades (Brierley, 2008)because of the large particle size of the marginal grade ore placed in them as well as inefficiencies in solution transport through the dump, and generally poor aeration that limits microbial activity (Brierley, 2008).

Heap leaching (Figure2.5) is similar to dump leaching but involves the construction of carefully designed heaps of low-grade ore in prepared areas. The ore is first crushed and then agglomerated, usually with sulphiric acid before being stacked in heaps up to 19 m high or less on pads lined with an impermeable barrier, such as a high-density polyethylene liner. The design of a heap operation may include aeration pipes which are added during construction to facilitate forced aeration to the heap, to ensure an aerobic environment in which the microbes are able to thrive. The ore is irrigated with acidic raffinate, while Inorganic nutrients such as $(NH)_4SO_4$ and KH_2PO_4 are frequently added to the raffinate prior to irrigation through drip lines placed on the surface of the heap. The leaching solution which passes downward through the heap and dissolves the elemental metals from the ore is known as the pregnant leach solution(PLS) which is collected at the bottom of the pad. The PLS is then directed to a series of processes which may include solvent extraction and or electrowinning. Also, the PLS may be recycled to the top of the heap, as an ‘intermediate’ leach solution (Rawlings, 2002, Gahan et al., 2012, Brierley, 2008). Compared with tank reactors, heap reactors are more difficult to aerate efficiently and the undesirable formation of gradients of pH and nutrient levels as well as liquor channeling are difficult to manage (Rawlings, 2005).

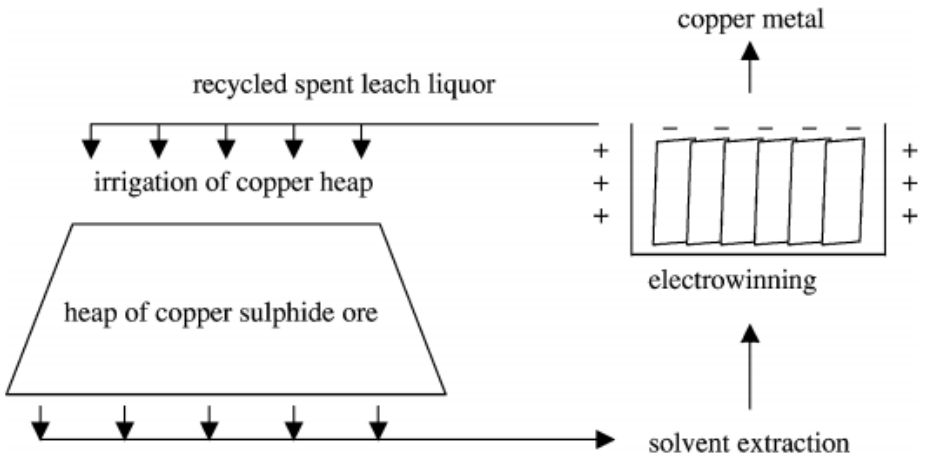

Figure 2.5: Schematic diagram of heap leaching (Rawlings, 2002)

2.4 Formation of Ferric ion precipitates

During microbial oxidation of ferrous ion, ferrous ion is oxidised to ferric ion by iron-oxidizing microbes, as seen in Eq. 2.5. The formation of ferric ion during microbial oxidation of ferrous ion is very crucial as it plays the role of a critical leaching reagent. The formation of ferric ion is acid-consuming which results in an increase in pH of the medium (Nemati et al., 1998). Ferric ion is sparingly soluble at higher pHs of about 2.5 (Grishin et al., 1988b) and readily precipitates as hydroxides, oxyhydroxides and hydroxysulphate (jarosite) compounds (MacDonald and Clark, 1970). The pH increase due to consumption of hydrogen ions is counteracted by the hydrolysis of ferric ion (Daoud and Karamanev, 2006) and stabilizes at pH values between 2 and 2.5 (Nemati et al., 1998)

$$Fe^{3+} + H_2O \leftrightarrow FeOH^{2+} + H^+ \quad 2.37$$

$$Fe^{3+} + 2H_2O \leftrightarrow Fe(OH)_2{}^{+} + H^+ \quad 2.38$$

$$Fe^{3+} + 3H_2O \leftrightarrow Fe(OH)_3{}^{2+} + 3H^+ \quad 2.39$$

Reactions 2.37 – 2.39 are highly influenced by the pH of the medium and therefore the pH of the medium has an influence on both the extent of oxidation and hydrolysis reaction (Liu et al., 2009). Jensen and Webb (1995) reported a competing reaction with the hydrolysis reactions (2.37 – 2.39) giving products of basic ferric hydroxysulphates, called jarosite compounds, with the formula $MFe_3(SO_4)_2(OH)_6$, which is an acid generating reaction, where M refers to a

monovalent cation such as K^+, Na^+, NH_4^+ and H_3O^+. These hydroxysulphates precipitates are known as jarosites which form according to the following reaction (Daoud and Karamanev, 2006),

$$3Fe^{3+} + M^+ + 2HSO^- + 6H_2O \rightarrow MFe_3(SO_4)_2(OH)_6 + 8H^+ \quad 2.40$$

Reaction 2.40 results in various forms of ferric ion precipitates (Table 2.4 below). The nature of the precipitate depends on the type of cation, M^+, which is present in abundance in the medium solution (Nazari et al., 2014, Daoud and Karamanev, 2006). Grishin et al. (1988b) suggest that elimination of these cations in the medium can reduce the amount of ferric ion precipitate formed.

Liu et al. (2009), studied the formation of jarosite by *Thiobacillus ferrooxidans* in ammonium-rich medium and confirmed the formation of ammoniojarosite, $(NH_4)Fe_3(SO_4)_2(OH)_6$. Also, Nazari et al. (2014) studied the formation of jarosite and its effect on crucial ions for *Acidithiobacillus ferrooxidans* in potassium rich medium and, from the XRD and SEM analysis, reported the formation of potassium jarosite, $KFe_3(SO_4)_2(OH)_6$. The XRD results obtained by Grishin et al. (1988b) in their study on characterization of jarosite formed in packed bed reactor, inoculated with *Thiobacillus ferrooxidans,* showed no evidence of ammonium traces despite the abundance of NH_4^+ in the medium which led to the authors reporting a mixed jarosite of K^+ and NH_4^+. This might have been attributed by the preferential precipitation of potassium jarosite over ammonium jarosite (Kaksonen et al., 2014b).

This controversy questions the submissions made by Nazari et al. (2014) and Daoud and Karamanev (2006) that the cation present in abundance determines the nature of the precipitate. Grishin et al. (1988b) suggested that hydronium jarosite, $(H_3O)Fe_3(SO_4)_2(OH)_6$, can only be synthesized in the absence of an alkali in the temperature range of 25 to 175^0C. In the presence of insufficient concentrations of cations, the ferric ion precipitates formed are composed entirely of schwertmannite, (Gramp et al., 2008).

Table 2.4: List of different forms of ferric ion precipitates and their chemical formula (Dutrizac and Jambor, 2000)

Formula	Mineral name	Synthetic equivalent
$KFe_3(SO_4)_2(OH)_6$	Jarosite	Potassium-hydronium jarosite
$NaFe_3(SO_4)_2(OH)_6$	Natrojarosite	Sodium jarosite
$RbFe_3(SO_4)_2(OH)_6$	No mineral equivalent	Rubidium jarosite
$AgFe_3(SO_4)_2(OH)_6$	Argentojarosite	Silver jarosite
$(NH_4)Fe_3(SO_4)_2(OH)_6$	ammoniojarosite	Ammonium jarosite
$TlFe_3(SO_4)_2(OH)_6$	Dorallcharite	Thallium jarosite
$PbFe_6(SO_4)_4(OH)_{12}$	Plumbojarosite	Lead jarosite
$HgFe_6(SO_4)_4(OH)_{12}$	No mineral equivalent	Mercury jarosite
$Pb\ (Fe,CU)_3(SO_4)_2(OH,H_2O)_6$	Beaverite	Lead copper jarosite
$(H_3O)Fe_3(SO_4)_2(OH)_6$	hydronium jarosite	Hydronium jarosite

Apart from various jarosites and ferric ion hydrolysis products, ferric ion complexes with sulphate and ferric precipitates of phosphates and oxy-hydroxides will occur (Nemati et al., 1998), which are amorphous and are of poorly defined mixture (Lazaroff et al., 1982).

2.4.1 Initial stage of formation of ferric ion precipitate

According to Pina et al. (2005) precipitation of ferric ion starts at pH 2. This was challenged by Córdoba et al. (2008b) who found that the precipitation of ferric ion was pronounced at pH as low as 0.9. According to Liu et al. (2007), the precipitation of ferric ion begins when microbes undergo their logarithmic growth phase. This was questioned by the findings of Liu et al. (2009) which revealed that the precipitation of ferric ion begins when the concentration of ferric ion in solution starts to decrease and this was evident long after logarithmic growth phase started. From the results reported by Liu et al. (2009), it can be hypothesized that the initial formation stage of ferric ion precipitation begins when the microbes reach their peak in a logarithmic growth phase and this can be perceived by the subsequent decrease in concentration of the ferric ion.

Sasaki and Konno (2000) proposed the initial formation stages of ferric ion precipitation to proceed in three distinct steps, which are: (1) the oxidation of Fe^{2+} by iron-oxidizing microbes to Fe^{3+}, (2) the formation of crystal nuclei (embryo) and lastly, (3) the growth of crystals of jarosite-type compounds.

Although Lazaroff et al. (1982), claimed that jarosite-type compounds were unlikely to be the primary products of microbial oxidation and suggested the formation of polymeric intermediaries to be precursors for jarosite however, Grishin et al. (1988b) later argued that jarosite-type compounds form directly from solution without a precursor solid phase. Furthermore, It was later reported by Casas et al. (2000), that jarosite formation starts from iron hydroxides, ($Fe(OH)_3$), formed by hydrolysis of ferric ion (Eq. 2.37 -2.39). While Jiang and Lawson (2004), later suggested that the formation of jarosite begins with species $FeSO_4^+$ and ($Fe(OH)_3$), elaborating the results of Casas and co-workers. However, the authors were uncertain about their result that they also suggested $[Fe(OH)_2]_2SO_4$ and $Fe(OH)SO_4$ to be precursors for the formation of jarosite. These inconclusive findings initiated the need to further extend investigations on understanding the precursor species of ferric ion precipitate.

It was in 2006 that Wang et al. (2006b) reported schwertmannite to served as a precursor solid for jarosite formation. Their findings, however, were contradicted by Córdoba et al. (2008a) who suggested goethite (FeOOH) to be the activating agent in the formation of jarosite. It is important to note that there is still no mutual consensus as to which species serve as precursor for jarosite and for this reason the effects of these precipitates on both microbial ferrous ion oxidation and bioleaching cannot be firmly understood, as it could be that the effects vary from primary precursor to primary precursor. Hence, the inconsistencies in published data create the need for further research. It may be possible that the type of primary species depends on the prevailing conditions. Studies that are directed at tracking down the primary products of ferric ion precipitates at different operating conditions are still required.

2.4.2 The effect of ferric ion precipitates on bioleaching and microbial oxidation of ferrous ion

The formation of ferric ion precipitates during microbial oxidation of ferrous ion may have adverse effects on process kinetics and biological processes (Daoud and Karamanev, 2006). Such adverse effects could include, blockage of pumps, reduction of the available ferric ion in solution required for metal sulphide attack, hinders transfer of substrates and metabolites as well as the creation of kinetic barriers caused by diffusion of reactants and products through the precipitation zone (Daoud and Karamanev, 2006, Meruane and Vargas, 2003, Smith et al., 1988, Liu et al., 2009). Moreover, there have been recent reports that ferric ion precipitates also affect the availability of ions required for nutrients by bacteria (Nazari et al., 2014).

Prior to these recent reports, Curutchet et al. (1992) had presented the view that ferric ion precipitates had no effect on the growth of *Thiobacillus ferrooxidans.* While Meruane and Vargas (2003) claimed that the inhibition of ferrous ion oxidation activity by *Acidithiobacillus ferrooxidans* was linked to the formation of ferric ion precipitate in solution. Also, Pina et al. (2005) and Mousavi et al. (2006), reported similar negative effects. Although Chowdhury and Ojumu (2014) claimed that the presence of ferric ion precipitate served as carrier matrix for microbial cells and actually enhanced the oxidation rate of ferrous ion by nearly 38%. However, Liu et al.(2017) recently presented findings that are contrary to theirs, as the authors reported higher pyrite biooxidation rates upon removal of the passive layer (jarosite).

The formation of ferric ion precipitates in bioleaching operations decreases the leaching efficiency by trapping the desired metal. This was witnessed in a study by Nheta and Makhatha (2013), where a recovery of 27% of nickel from the treatment of jarosite was achieved.

Córdoba et al. (2008a) stated that controlling the formation of ferric ion precipitate could be very difficult to achieve since the precipitation occurs spontaneously. It is reported that in the absence of excessive ferric ion precipitation, the microbial oxidation of ferrous ion becomes the principal rate-limiting step in the overall process of bioleaching (Smith et al., 1988).

2.4.3 Factors affecting the formation of ferric ion precipitate

Ferric ion precipitation is affected by various factors such as temperature, pH, time, ferrous ion concentration, agitation speed, alkali concentration, reactor type and jarosite seed. However, for the purpose of this study, the discussion will be limited to pH and temperature.

The effect of ferrous ion on the formation of ferric ion precipitate is still under debate. For instance, Córdoba et al. (2008a) reported that ferrous ion was responsible for the formation of both jarosite nuclei and ferric ion precipitate, while Zhu et al. (2008) argued that the presence of ferrous ion prevented the formation of both nuclei and ferric ion precipitate.

2.4.3.1 Effect of pH

Daoud and Karamanev (2006), studied the effect of temperature and pH on ferric ion precipitation and reported pH to be the main parameter affecting ferric ion precipitate formation. The authors reported an optimal pH range of 1.6 - 1.7 giving least amount of ferric ion precipitation of 0.0125 – 0.0209 g. Liu et al. (2009) reported similar optimum pH giving ferric ion precipitate concentration of 3.37 g/L. It should be noted, however, that both studies were conducted in shake flasks and for short duration to have allowed prominent precipitation and

according to Margulis et al. (1976), jarostic complex form slowly and incompletely at pH range of 1.8 – 2.7.

In a recent study by Nazari et al. (2014), it was reported that maximum quantity of ferric ion precipitated at pH above 2.2. Ojumu and Petersen (2011), studied the effect of pH on the kinetics of ferrous ion oxidation by *Leptospirillum ferriphilum* and reported the precipitation of ferric ion to be significant beyond pH 1.3. Interesting results were found by Wanjiya et al. (2015) where the authors reported a 33% and 52% reduction in the mass of ferric ion precipitate upon subsequent reduction of pH from 1.7 to 1.5 and 1.3 respectively after operating for 10 days. It is quite evident that the pH of the medium plays a crucial role in the formation of ferric ion precipitate.

2.4.3.2 Effect of Temperature

Substantial evidence exists that ferric ion precipitation is significantly dependent on temperature (Nemati et al., 1998). It is well believed that precipitation of ferric ion is more rapid and complete as the temperature increase (Lazaroff et al., 1982) and that there is temperature-dependency of the rate of ferric ion precipitation (Bigham et al., 2010).

Leduc et al. (1993) studied the characterization of ten different isolates of *Thiobacillus ferrooxidans* in the temperature range 2 – 35^{0}C and reported minimal ferric ion precipitation at temperatures less than 10^{0}C. Also, a minimal formation of ferric ion precipitate was reported at 35^{0}C by Daoud and Karamanev (2006). Bigham et al. (2010), investigated the characterization of jarosites produced by chemical synthesis over a temperature range of 2 to 40^{0}C and found the precipitation of ferric ion to increase with temperature. Wang et al. (2006a), found that schwertmannite transformed to jarosite upon increasing temperature from 36 to 45^{0}C. The effect of temperature on ferric ion precipitation, whatsoever, cannot be studied independently because it is affected by pH. This is because ferric ion precipitation at higher pHs is minimized at lower temperatures (Daoud and Karamanev, 2006). This was confirmed by Ongendangenda and Ojumu (2013) where the authors reported minimal ferric ion precipitation at the same pH range investigated by Ojumu and Petersen (2011) but at lower temperatures.

2.5 Summary

Bioleaching has been proven to be more efficient than conventional processes due to its simplicity and applicability to low-grade ore. Extensive studies have been conducted to optimize bioleaching with respect to its operating parameters as well as understanding the kinetics thereof.

Over the past years, studies directed at quantifying ferric precipitate have been conducted, however, these studies were conducted in shake flasks which do not simulate real bioleach systems. The short duration employed in these studies invites the possibility of the microbes being in their lag phase when the experiments were conducted as well as the possibility of ferric ion, which is a major source required for precipitation, not being produced to considerable amounts to have allowed significant precipitation. Smith et al. (1988), insinuated that the factors which affect microbial oxidation of ferrous ion to ferric ion will directly impact the precipitation of ferric ion. Moreover, as seen in Daoud and Karamanev (2006), reactor type is one of these factors. For this reason, quantification studies in systems such as CSTR, that can simulate real bioleach systems are necessary.

As reviewed above, it should be noted that most quantification studies were conducted employing *Acidithiobacillus ferrooxidans* which is a strain believed to be less tolerant to high concentrations of ferric ion. Due to the interest that *Leptospirillum ferriphilum* has attracted in the context of understanding the kinetics of microbial oxidation, it is important to understand its role in the quantification of ferric ion as well so as to provide a data base.

The only knowledge that exists on ferric iron precipitates e.g jarosite is limited to their mineralogy, physical and chemical characterization. This is only helpful in understanding the nature of the precipitates but does not provide an understanding of the interactions of ferric iron precipitates with process kinetics and how valuable metals adsorb onto precipiates. Therefore, this study tries to provide an understanding of surface properties of ferric-ion precipitates with a view to investigate the effects of initial solution pH on the quantification and surface properties of ferric ion precipitates formed during microbial oxidation of ferrous ion. This understanding will be useful in the design of bioleaching operation that minimizes both the loss of valuable metals and quantity of ferric iron precipitate.

Chapter 3

MATERIALS AND METHODS

This chapter presents a detailed description of the materials used during the experiments, as well as the experimental approach adopted to achieve the study's objectives. It also includes a detailed description of the experimental methods and the analytical techniques employed for the study.

3.1 Materials

3.1.1 Experimental rig

The batch experiments were conducted in a single 2 L jacket stirred tank bioreactor, which had a working volume of 1 Litre and is also made of borosilicate glass (Figure3.1) fitted with a top with four ports to allow insertion of blade agitator, air sparger, condenser and a sampling point. Attached to the reactor was an FMH model TR-E constant temperature water bath, which maintained the desired temperature within the bioreactor by circulating water through the bioreactor jacket. Mixing and gas dispersion was achieved by a pitched (60^0) three-blade turbine impeller located approximately 2 cm from the base of the reactor. Air was supplied by a Watson-Marlow 101U/R compressor and the gas flow rate was controlled using a bubble air flow meter. The solution's reduction-oxidation (redox) potential and pH was analysed using a CRISON GLP 21 redox and pH meter. Evaporation was minimized by the use of a condenser which was connected to a chiller operated at 6 ^{0}C.

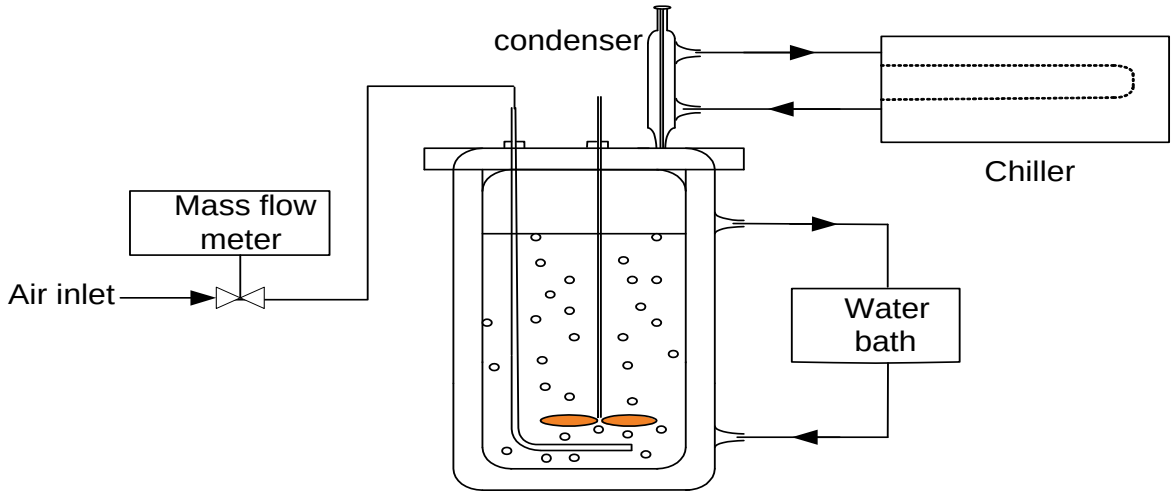

Figure3.1: Diagrammatic representation of experimental rig

3.1.2 Growth medium

Analytical grade reagents were used for all the experiments. The ferrous media consisted of the desired quantity (in $g.L^{-1}$) of Fe^{2+} (added as $FeSO_4$. $7H_2O$), 1.11 K_2SO_4, 1.83 $(NH_4)_2SO_2$, 0.53 $(NH_4)_2HPO_4$ and 10 mL of Vishniac solution, a trace element solution (Vishniac and Santer, 1957), adjusted to the desired pH ($0.7 \leq pH \leq 1.30$) using concentrated H_2SO_4. No attempt was made to maintain sterile conditions. In order to prepare the Vishniac solution, 15 $g.L^{-1}$ EDTA ($C_{10}H_{14}N_2Na_2O_8.2H_2O$, M = 372.24 $g.mol^{-}$) was dissolved in 200 mL of 6% (w/v) KOH solution. In a separate container, 22 g $ZnSO_4.7H_2O$, 9.24 g $CaCl_2.2H_2O$, 5.06 g $MnCl_2.4H_2O$, 5.0 g $FeSO_4.7H_2O$, 1.1 g $(NH_4)_6Mo_7O_{24}.4H_2O$,1.58 g $CuSO_4.5H_2O$, 1.62 g $CoCl_2.6H_2O$ were added to 400 mL dH_2O. Each component had to be completely dissolved before the addition of the EDTA solution and the Vishniac solution and made up to 1 L with sterile distilled water. The resulting solution was stored in a fridge to prevent oxidation of ferrous ion.

3.1.3 Bacterial culture

The inoculum was obtained from a vat-type two-stage (2 × 20 L) continuous bioleaching mini-plant treating a pyrite-arsenopyrite concentrate, in Gamsberg, South Africa. After isolation of the ferrous ion oxidising species, *Leptospirillum ferriphilum* sp. Nov., was found to be the only iron oxidising species (Coram and Rawlings, 2002). The stock culture was maintained in a continuous stirred tank reactor maintained at 35 ^0C at a residence time of 40 hours on a feed solution containing 12 $g.L^{-1}$ as total iron.

3.2 Methods

3.2.1 Experimental approach

Batch culture experiments with *L.ferriphilum* were carried out in a CSTR bioreactor with a working volume of 1L. The bioreactor was maintained at the desired temperature using a constant temperature water bath. The solution was aerated with dry air at a flow rate of 3mL.s^{-1} while the off-gas was passed through a condenser to minimize evaporation.

The pH of the solution in the bioreactor was not controlled directly; however, the desired pH was obtained by setting the initial pH to the desired pH.

A set of three reactors were operated at any given time of the day at the same operational conditions and the results were averaged. New experiments were initiated by mixing 20% of inoculum (obtained from a continuous system with redox potential above 600mV) with 80% of growth medium. The bioreactor was cleaned after each experimental condition with concentrated HCl (32%). This ensured the complete removal of ferric precipitate and any wall growth. The bioreactor was then washed with diluted H_2SO_4 (50%) to remove the HCl, which is detrimental to microorganisms. Finally, the bioreactor was rinsed with distilled water to neutralize the pH in the reactor.

3.2.2 Experimental study on the effect of operating pH on the amount of precipitate formed

Batch culture experiments with *L. ferriphilum* were carried out in a CSTR bioreactor, as shown in Figure 2.6. The cell suspension was aerated with dry air at a flow rate of 3 mL.s^{-1}. The initial pH of the solution medium was varied at 1.3, 1.5, 1.7, 1.9 and 2.2 using concentrated H_2SO_4 while the temperature was kept constant at 35 ^{0}C using a controlled temperature water bath. The solution was agitated at 350 – 400 rpm. The bioreactor was allowed to operate for 14 days and an analysis of total iron, ferrous ion, pH and redox potential were performed daily.

3.2.3 Characterization of ferric ion precipitates

The ferric ion precipitates were collected at the termination of each experiment after two weeks by sedimentation followed by filtration with a vacuum pump using Whatman polycarbonate filters. The precipitates on the filter paper were washed back to the reactor using 0.1 N sulphiric acid, while precipitate on the walls of the reactor and the precipitate that attached to the surfaces of the air sparger as well as the impeller was stripped with 100 mL of 0.1 N sulphiric acid. The resulting solution was allowed to settle for 3 hours before it was decanted, and the

precipitate-containing portion was filtered (Grishin et al., 1988b). The final product was washed with diluted H_2SO_4 (5%) and distilled water to remove any remaining medium and dissolved ions (Daoud and Karamanev, 2006). The precipitates were dried at 104 ^{0}C overnight to a constant weight (Grishin et al., 1988b) and the final product was sent for analyses.

3.2.4 Adsorption experiments

Adsorption experiments were performed with 1 g precipitate in 100 mL of NaCl solution, with the ionic strength of 10^{-3} mol/L at similar pH at which the precipitate was formed (1.3 – 2.2) to simulate the solution chemistry of the biooxidation experiments. The solution contained an initial copper concentration of 0.5 g/L. The experiments were carried out in Erlenmeyer flasks which were placed on a Thermostat Orbital shaker. The mixture was agitated at 200 rpm at 35 ^{0}C for 3 days, however, equilibrium studies were not conducted in this study. The amount of copper adsorbed was determined by subtracting the concentration of copper at the end of the experiment from the initial concentration. Concentrations of copper were determined by Atomic Absorption Spectroscopy (AAS). After conditioning, the suspension was filtered to separate the solids which were then sent for zeta potential measurements. The change in magnitude of the surface charge of the precipitate, before and after adsorption experiments, was used as a proxy measure for the amount of copper adsorbed onto the precipitate.

3.3 Analytical procedure

Distilled water and analytical grade laboratory chemicals were used for all the experiments.

3.3.1 Iron determination and quantification

Samples were collected daily and measured for mass balancing purposes. The redox potential of the solution in the bioreactor was measured daily using a redox electrode (Ag/AgCl). The redox probe was calibrated regularly before any measurements under the same conditions as the bioreactor. This allowed the determination of ferric-to-ferrous ion ratio in the bioreactor solution (refer to section 3.3.2). The total iron [Fe^{tot}] concentration was determined by titration with potassium dichromate using the BDS indicator (Svelha, 1996). The concentrations of ferric ion and ferrous ion were calculated from the values of [Fe^{tot}] and Eh at each time during the experiment using the following expressions:

$$R = \frac{[Fe^{3+}]}{[Fe^{2+}]} = 10^{\left(\frac{Eh-463.8}{24.45}\right)} \qquad 2.44$$

$$[Fe^{2+}] = \frac{[Fe^{tot}]}{1+R} \quad 2.45$$

$$[Fe^{3+}] = [Fe^{tot}] - [Fe^{2+}] \quad 2.46$$

The total iron concentration in the system was assumed to be constant throughout the investigation. Ferric ion precipitation was used as a proxy measure of the iron loss during the process, and this was determined at the end of each experimental run. The liquid in each bioreactor was filtered using a vacuum flask and filter paper (25 µm pore size). The solids on the filter paper were returned to the corresponding bioreactor by washing with concentrated hydrochloric acid. HCl readily dissolves the filtered jarosite and that attached to the wall of the bioreactor. Finally, the precipitate was measured as total iron concentration by dissolving samples in concentrated HCl prior to measurement by using an atomic absorption spectrophotometer (Ongendangenda and Ojumu, 2013). To get the accumulated precipitate in grams, the concentration value reported by Atomic Absorption Spectrometer was multiplied by the working volume of the solution.

3.3.2 pH and redox potential measurements

The pH and redox potential were measured using a CRISON GLP 21 pH/Eh meter instrument. The pH electrodes were calibrated at pH 4, 7 and 9 using buffer solutions from Merck before every measurement.

The redox electrode (i.e., Ag/AgCl electrode) was calibrated against the half reaction of ferrous to ferric oxidation ($Fe^{2+} \rightarrow Fe^{3+} + e$) which was the only redox couple existing within the bioreactors. The calibration was performed at the experimental condition and the calibration curve was plotted using the Nernst equation as shown in Equation 2.47. This enabled the determination of $[Fe^{3+}]/[Fe^{2+}]$ in the bioreactors.

$$E_h = E_h' + \frac{RT}{nF} ln \frac{[Fe^{3+}]}{[Fe^{2+}]} \quad 2.47$$

Where E_h is the standard redox potential and $[Fe^{3+}]/[Fe^{2+}]$ is the ratio (R) between the total concentration of ferric and ferrous ions. The term E'^h is defined as the solution potential measured at equal total ferric and ferrous ion concentration, which accounts for the activity coefficient, formation of complexes, electrode type and fouling of the electrode. E'^h values

may be determined from the intercept of the plot E_h versus ln ($[Fe^{3+}]/[Fe^{2+}]$), while the slope gives RT/nF (Chowdhury, 2014)

3.3.3 Precipitate characterization

The precipitates were obtained at termination of each experimental run. Chemical and micro-structural analyses were conducted using X-ray diffraction (XRD) and scanning electron microscopy (SEM). Energy-dispersive X-ray spectrometry (EDX, employing an EDAX® analytical EDX system with SEM-EDS internal standard) was used for semi-quantitative elemental analysis of the precipitate.

3.3.4 Particle size distribution measurement

The particle size distribution of the precipitates was measured using laser diffraction techniques (Malvern Mastersizer, MS S LB model and Malvern Zetasizer, Nano ZS model).

3.3.5 Zeta potential measurements

The zeta potential of the precipitates was measured using a dynamic back light scattering technique (Malvern Zetasizer, Nano ZS model).

Chapter 4

Effect of initial solution pH on the formation of ferric ion precipitate during ferrous ion oxidation by *Leptospirillum ferriphilum*

4.1 Introduction

Bioleaching has emerged as an alternative technology in the extraction of low-grade ores, especially copper and gold, due to its operational simplicity and environmental advantages. It offers a great number of advantages over conventional processes. However, in order for bioleaching to outperform conventional processes, it needs to be optimized with respect to operating conditions and reaction kinetics. Optimization of bioleaching is in direct relation with optimization of its sub-processes. Biooxidation has been perceived to be the cardinal subprocess of bioleaching (Wanjiya, 2013, Mousavi et al., 2006).

Biooxidation involves the oxidation of ferrous ion to ferric ion which is a critical reagent in bioleaching operation (Chowdhury, 2014). However, depending on solution conditions; especially solution pH, ferric ion readily precipitates into amorphous ferric ion precipitates of different forms. The precipitation of ferric ion is undesired because of its interference with process kinetics and it is an inevitable phenomenon. Although relatively low pH conditions (<0.9) have been reported to minimize ferric ion precipitation (Córdoba et al., 2008b), they become very significant over the long term (Grishin et al., 1988b). This is because ferric ion precipitates have been perceived to pose negative impacts on both biooxidation and bioleaching, therefore, as recently recommended by Chowdhury (2014), its management during operation is vital.

Smith et al. (1988), postulated that in the absence of excessive iron precipitation, the microbial oxidation of ferrous ion becomes the principal rate-limiting step in the overall process of microbial leaching of mineral ores. The authors further stressed that the leaching medium must be maintained to enhance the process of indirect microbial leaching with ferric ion by preventing ferric ion precipitation, while also maintaining conditions to allow for efficient microbial oxidation of ferrous ion to ferric ion. For this reason, it is evident that studies directed at managing the formation of iron precipitate during biooxidation of ferrous ion are crucial to enhance process kinetics.

For the past decades, studies directed towards quantifying ferric ion precipitates have been performed (Meruane and Vargas, 2003, Daoud and Karamanev, 2006, Liu et al., 2009). However, these studies were conducted in shake flasks which do not simulate real heap systems and were conducted for short cultivation time to have allowed significant precipitation e.g. 48h in the study of Daoud and Karamenev (2006). It is reported that iron precipitates such as jarosite complexes form slowly and incompletely at low pH (Lazaroff et al., 1982). Therefore, the results from these studies are meaningless on industrial scale where reactor volumes range from 440 – 21600 m^3 (Rawlings et al., 2003) and operations go for as long as 1 year (Watling et al., 2009), especially with the difficulties encountered by scientists, on how to turn lab scale research into full-scale operation by scaling up the research (Gahan et al., 2012).

Smith et al. (1988), proposed that factors which affect microbial oxidation of ferrous ion to ferric ion will directly impact the precipitation of ferric ion and according (Daoud and Karamanev, 2006)) reactor configuration was amongst the factors which affect microbial oxidation. Heaps and stirred tanks are two different engineering applications that are mostly applied and implemented in bioleaching and biooxidation (Tao and Dongwei, 2014), therefore, ferric ion precipitate quantification studies in systems such as CSTR are required.

It is widely reported that the role of microorganisms during microbial oxidation of ferrous ion is to act as a biocatalyst (Mousavi et al., 2006, Coram and Rawlings, 2002). However, it should be noted that majority of the quantification studies utilized *Acidithiobacillus ferrooxidans* as a biocatalyst. One of the requirements for iron precipitation is that the solution medium must be reached in ferric ion (Liu et al., 2009), and *Acidithiobacillus ferrooxidans* have been perceived to be inhibited by ferric ion (Nyavor et al., 1996). Whereas *leptospirillum ferriphilum* is less sensitive to ferric ion (Rawlings et al., 1999), moreover, it is kinetically favoured due to its dominance in stirred bioreactors (Kaksonen et al., 2014a). Over the past decades and more recently, *Leptospirillum ferriphilum* has gained interest and has been widely used in investigating the kinetics of ferrous ion oxidation (Ojumu et al., 2008, Ongendangenda and Ojumu, 2013, Breed and Hansford, 1999, Ojumu, 2008, Nazari et al., 2014, Wanjiya, 2013, Chowdhury and Ojumu, 2014, Ojumu and Petersen, 2011, Van Scherpenzeel et al., 1998, Ojumu et al., 2009). Therefore investigations of quantification studies biocatalysed by *Leptospirillum ferriphilum* are of much interest.

Most quantification studies are with respect to pH, temperature and time while the effect of redox potential on the amount of ferric ion precipitate during microbial oxidation has been less

investigated. Córdoba et al. (2008a), were the first to propose that the precipitation of ferric ion is directly related to the redox potential of the solution. The authors believed that significant precipitation of iron occurred at redox potentials higher than the critical value (between 400 and 500 mV). It is, therefore, important to investigate the effect of redox potential on the amount of iron precipitate formed.

This chapter is a presentation of the results for the quantification of iron precipitate during microbial oxidation of ferrous ion mediated by *Leptospirillum ferriphilum* in a CSTR as a function of pH (1.3 – 2.2) and time (5 – 14 days). This study is aimed at developing a database of the effect of initial solution pH on the amount of ferric ion precipitate formed during biooxidation. The outcome of this study will help gain insight on how initial solution pH affects the amount of iron precipitate over time on a larger scale which prevails in hydrometallurgy operations. This may assist in the management and operation of full-scale bioleaching and biooxidation processes.

4.2 Experimental procedure

Quantification studies were carried out in a CSTR operated at 35 ^{0}C and at varying pHs of 1.3, 1.5, 1.7, 1.9 and 2.2 and as a function of time 5, 8, 12, 14 days. The experimental design and experimental procedure used in this study are outlined in sections 3.1.1 and 3.3.1

4.3 Results and discussion

4.3.1 Changes in redox potential and pH

The changes in redox potential at different initial pH from 1.3 – 2.2 with time are shown in Figure 4.1. The changes in the redox potential can directly be linked to the oxidation of ferrous ion by the microorganisms (Third et al., 2000). Since the increase in redox potential is linked to increase in oxidation of ferrous ion (Tekin et al., 2013) it can be seen that higher oxidation rates and higher production rate of ferric ion were achieved at pHs 1.7, 1.9 and 2.2. It can be seen that maximum oxidation was achieved in less than 4 days under these initial pHs. The slow increase in redox potential at initial pH of 1.3 and 1.5 represents the slow metabolize of *Leptospirillum ferriphilum* in the lag phase resulting in slow oxidation rates of ferrous ion which is related to the inhibition of the bacterial activity by acidity. It is evident that if initial rates were to be determined at 22 h and 46 h, as done by Daoud and Karamanev (2006), high oxidation rates would be achieved at pHs 1.7, 1.9 and 2.2 respectively since almost all the ferrous ion has been oxidised. This result may be corroborated by the optimum pH for *Leptospirrilum feripillum* of 1.8 reported by Rawlings (2002).

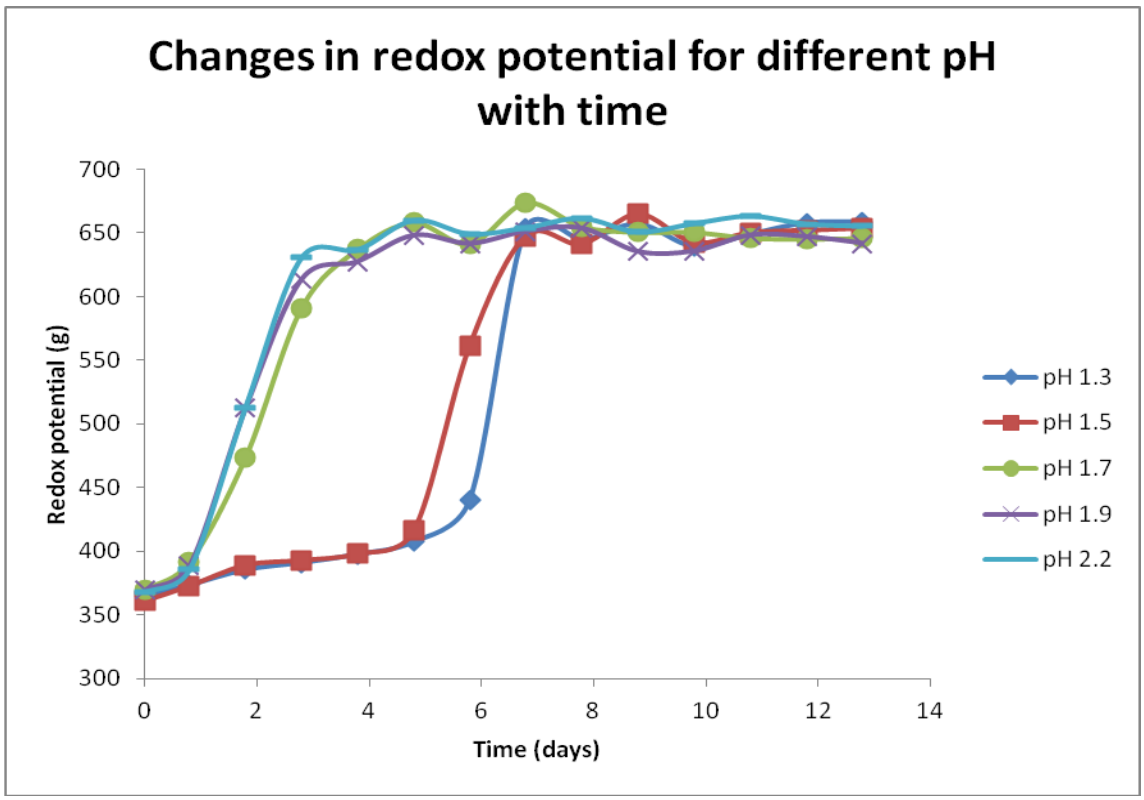

Figure 4.1: Changes in redox potential at different initial pH with time

The changes in solution pH at different initial solution pH with time are depicted in Figure 4.2. The general trend observed in the Figure is the increase in solution pH followed by a successive decrease in pH. The increase in pH is as result of the consumption of hydronium ions related to the oxidation of ferrous ion, while the decrease is attributed to the precipitation of ferric ion which is accompanied by the release of hydronium ion. The stabilizing pH for all the different initial pHs is found to be around 1.5. The same as the redox potential changes, the increase in solution pH can be related to the extent of ferrous ion oxidation (Qiu et al., 2005) since it is the only reaction responsible for increase in solution pH. It can be seen that the steady increase in pH at initial pH of 1.3 and 1.5 is attributed to the slow activity of the microbes under acidic conditions as was observed in Figure 4.1. Since the requirements for the decrease in solution pH is high concentration of ferric ion (Jin et al., 2013), it can be stressed that at initial pH of 1.7, 1.9 and 2.2 ferrous ions have completely oxidised after day 2 suggesting that the oxidation of ferrous ion at initial pHs of 1.7, 1.9 and 2.2 was almost complete on the second day leaving the medium rich in ferric ion.

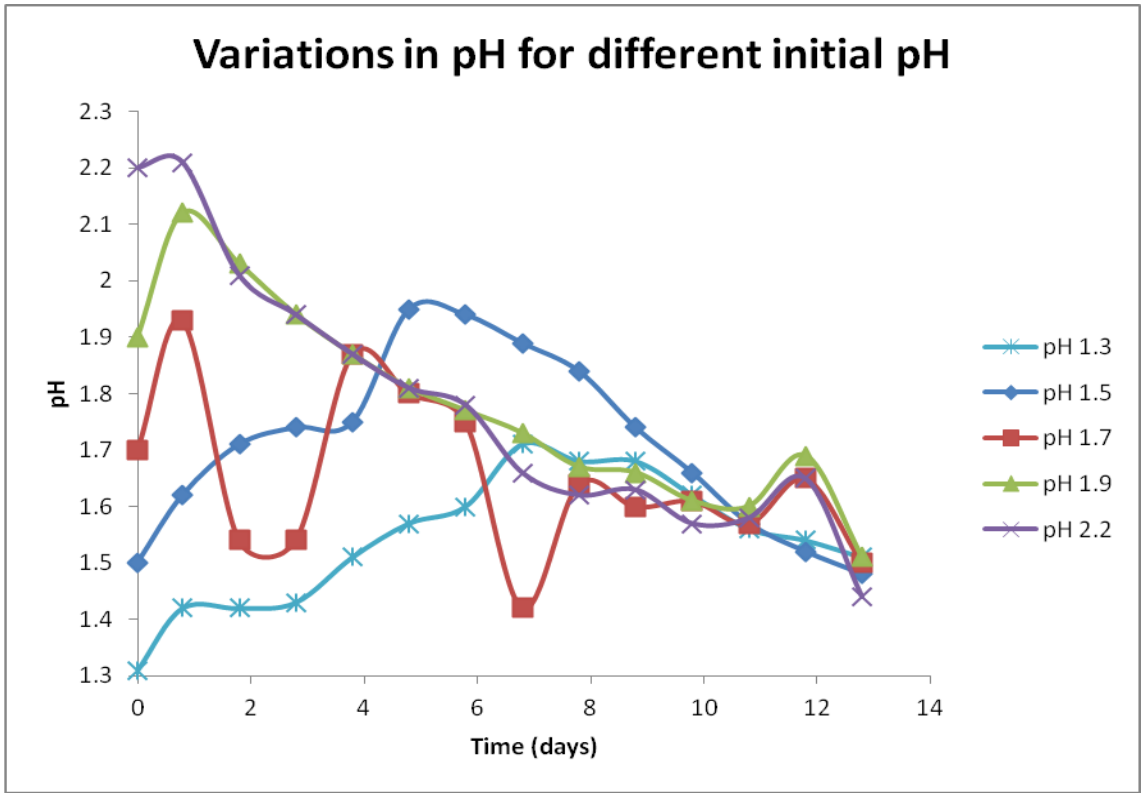

Figure 4.2: Changes in solution pH with time

4.3.2 Influence of initial pH on the mass of ferric ion precipitate

The relationship between iron precipitate mass and initial pH is shown in Figure 4.3. The general trend observed from the results is that the amount of iron precipitate increases with an increase in initial pH, as witnessed and reported by Liu et al. (2009) and Wanjiya et al. (2015). The least amount of iron precipitate was obtained at initial pH 1.3 (4.31 g), while initial pH of 2.2 gave the most iron precipitate (13.26 g). In a different study by Daoud and Karamanev (2006), no iron precipitate formation was reported at pH 1.6 and the most probable reason for this could be the short duration of time employed, which was 48 hours as compared to 14 days in this study. It is also probable that the strain used by the authors, *Acidithiobacillus ferrooxidans,* is not an effective biocatalyst as compared to *Leptospirillum ferriphilum* because significant losses of total iron at pH as low as 1.3 were reported in a medium biocatalysed by *Leptospirillum ferriphilum* (Ojumu and Petersen, 2011). The results in Figure 4.3 can be well explained by carefully examining the results from Figures 4.1 and 4.2.

Figure 4.1 can be used to relate the amount of ferric ion in solution medium and it is clear from the Figure that high concentrations of ferric ion were achieved early at higher pHs of 1.7, 1.9 and 2.2 as compared to pH 1.3 and 1.5. The large amounts of iron precipitate at pHs 1.7, 1.9 and 2.2, corresponds to the higher redox potential values which are within the critical values (400 – 500 mV) necessary for significant precipitation (Córdoba et al., 2008a). From this, it is proposed that the amount of iron precipitated is proportional to the time a solution medium which is rich in ferric ion is allowed to proceed, given that the redox potential is within the critical values. In Figure 4.2 above, it was stated that the decrease in solution pH was attributed to the subsequent precipitation of ferric ion. By carefully examining Figures 4.2 and 4.3, it can be suggested that the magnitude of the decreasing gradient in pH is proportional to the amount of iron precipitated. This can be used to explain the excessive mass of iron precipitated at pH> 1.7.

The mass of iron precipitate found in this study is comparably higher to the mass found in other studies (Nazari et al., 2014, Daoud and Karamanev, 2006, Wanjiya, 2013, Liu et al., 2007, Liu et al., 2009). A possible reason being the difference in the type of strain used (Coram and Rawlings, 2002) and reactor type (Daoud and Karamanev, 2006). These results support the hypothesis proposed by Smith et al. (1988). The type of strain has a pronounced effect on the formation of ferric iron precipitae, much more than could be realized. A recent study by Wanjiya et al. (2015), investigated the management of jarosite in a novel packed-column bioreactor inoculated with *Acidithiobacillus ferrooxidans* at similar pHs to this study and for a duration of 15 days, however in continuous mode. The mass of iron precipitate obtained at pH 1.7 was 5 g compared to 8.44 g. The discrepancy between these studies lies in the different strain used as well as the type of reactor used. Even though the authors used a larger working volume in comparison to the above studies, the working volume in this study was two times larger and hence the larger mass of iron precipitate.

Surprisingly, the precipitate mass of 4.31 g at pH 1.3 obtained in this study is much higher than that obtained by Grishin et al. (1988b) which is 0.41 g and at a similar pH, over a duration of 3 months. The obvious reason is that their study was conducted in a smaller volume of 50 mL, moreover, the system was continuous, hence, some of the precipitated iron was continuously removed from the system by the effluent stream.

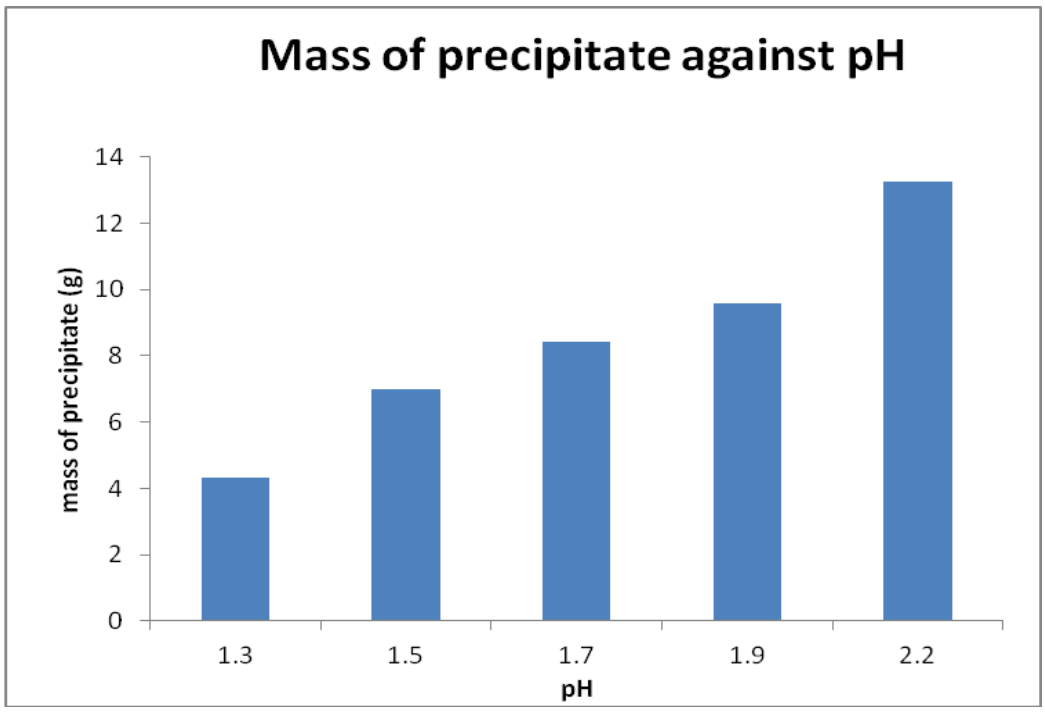

Figure 4.3: Mass of precipitate obtained after 14 days of operation at different initial pH

4.3.3 Effect of incubation time

Figure 4.4 shows the mass of precipitate obtained with time and the maximum redox potential reached at termination of the experiment with initial solution pH of 1.5. These experiments were conducted with the view of determining the range of redox potential at which significant iron precipitation occurs in batch systems. Figure 4.4 clearly shows that the mass of iron precipitated is proportional to the duration of operation. This trend is in accordance to the trend reported by Dutrizac and Jambor (2000). However, the results show that significant precipitation occurred during the 5th and 8th day of operation where the maximum redox potential varied from 403 to 624 mV. This range corresponds to the exponential phase of the microorganisms and substantiates the findings of Liu et al. (2007), where the authors reported that precipitation of ferric ion begun at the initial stage of exponential phase. Leaving the experiments to run for further 4 and 6 days after the 8^{th} day resulted in an increase in precipitation of 0.2 and 3.6 % respectively which was not significant.

From this, it can be concluded that significant precipitation occurs during the logarithmic growth phase of microorganisms, which is within the suggested critical redox potentials of 400 – 500

mV reported by Córdoba et al. (2008a). This implies that to minimize the accumulation of ferric ion precipitate in batch systems operating for prolonged duration, the redox potential should be above or below the critical values. The results further show that precipitation of ferric ion in batch systems beyond the exponential phase is insignificant, therefore, even if the system could be allowed to run for a longer period, no significant precipitation would be achieved. It is evident that excessive precipitation in continuous systems would be dominant since continuous systems are operated at exponential phase.

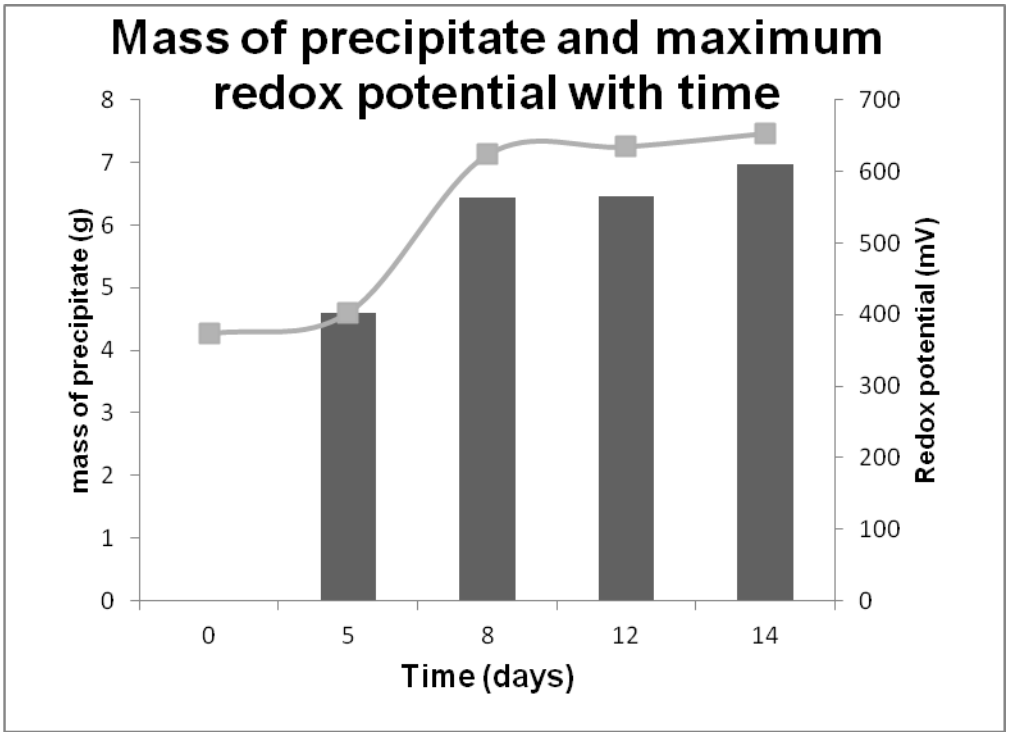

Figure4.4: The amount of iron precipitated (bar graph) and maximum redox potential (line graph) reached at termination of experiment with time at initial pH 1.5

4.4 Conclusion

The purpose of this study was to quantify ferric ion precipitate due to changes in initial solution pH of biooxidation medium and to investigate the role of redox potential on the amount of ferric ion precipitated. Even though there have been studies on this subject, there is still limited studies on quantitative measurement in the context of industrial scale situation. The results show that the amount of ferric ion precipitated is proportional to the initial solution pH.

Increasing the initial pH resulted in increased amount of iron precipitated. The amount of iron precipitated in this study is comparably higher to the reported amounts in literature simply because of the larger reactor volume used in this study and the type of microorganisms used which are less sensitive to high concentrations of ferric ion as compared to other microbes. The results show that significant iron precipitated during the exponential phase where the redox potential was within the critical values (between 400 and 500 mV) recommended by Córdoba et al. (2008a) for significant precipitation.

The insight gained in this study will help give an idea of the amount of iron precipitated in industrial scale where operations run for days, months and even years. It will also assist in the management of iron precipitates as well as its minimization, which is of practical importance in hydrometallurgy, where significant precipitation may be seen to be undesired. The study showed that even though low pH levels have been reported to minimize ferric ion precipitation, the amount of ferric ion precipitate formed in larger volume reactors and over a long duration become significant and cannot be ignored. It is expected that these results will give a somewhat indication of what to expect on an industrial scale.

Chapter 5

Effect of initial solution pH on surface properties of ferric ion precipitates

5.1 Introduction

Bioleaching has been proved to be the most efficient technology for the recovery of valuable metals from sulphide minerals. However, during bioleaching of sulphide minerals, there is a competing reaction that promotes the formation of different types of undesired ferric ion precipitates which are amorphous compounds and tend to have large surface areas. The formation of ferric ion precipitates is beneficial in processes where control of undesired iron and impurities is desired e.g zinc industries (Dutrizac, 1999). However, in bioleaching operations, ferric ion precipitation is undesired because of its negative implications (Daoud and Karamanev, 2006). These include, blockage of pumps, reduction of the available ferric ion in solution required for metal sulphide attack, hinder transfer of substrates and metabolites and the creation of kinetic barriers caused by diffusion of reactants and products through the precipitation zone (Daoud and Karamanev, 2006, Meruane and Vargas, 2003, Smith et al., 1988, Liu et al., 2009) and recently it has been reported that ferric ion precipitates also affect the availability of ions required for nutrients by bacteria (Nazari et al., 2014).

The formation of ferric ion precipitates in bioleaching operations also decreases the leaching efficiency by trapping the leached valuable metals in solution. A recent study by Nheta and Makhatha (2013), showed that about 27% of nickel can be recovered from jarosite precipitated from bioleaching. Even though the two-stage continuous stirred tank bioreactor (CSTR) proposed by Kaksonen et al. (2014b) could achieve efficient precipitation of ferric ion with minor co-precipitation losses of Cu and Ni, however, studies directed at investigating the surface properties of iron precipitates are of crucial importance. Also, they could help assist in understanding the adsorption abilities of iron precipitates and maybe the operating parameters could be manipulated to promote the formation of iron precipitates with surface properties of less adsorption abilities while maintaining higher rates of ferrous ion oxidation and higher recovery efficiencies.

Characterization studies of ferric ion precipitates have been reported extensively but only extends up to mineralogy, morphology, elemental composition (Kaksonen et al., 2014b, Chiranjit, 2013, Grishin et al., 1988b, Bigham et al., 2010, Nazari et al., 2014, Wang et al.,

2006b, Lazaroff et al., 1982, Pham et al., 2006, Toro et al., 1988, Liu et al., 2009). This information alone is not enough to completely understand the interactions of ferric ion precipitates with process kinetics and how these precipitates scavenge valuable metals. Therefore, more studies are still required to fully understand the surface properties with respect to the surface charge. It is anticipated that the adsorption characteristics of iron precipitate is influenced by the surface charge of the precipitate.

The objective of this study was to characterize and investigate the surface properties of ferric ion precipitates formed during ferrous ion oxidation by *Leptospirillum ferriphilum* in a CSTR as a function of initial solution pH 1.3 to 2.2. This understanding will help gain insight into the ability of the ferric ion precipitate to scavenge the desired metal, subsequently, this will improve recovery of valuable metals and sustainability in the Hydrometallurgical world. This study is conducted to establish a link between solution pH and surface charge of the precipitate and relate this surface charge to the adsorption of valuable metals onto iron precipitate.

5.2 Experimental procedure

The reactor set-up, analytical techniques and experimental procedures used in this study are described in detail in Sections 3.1.1, 3.2.1, 3.2.2, 3.2.3 and 3.3.

5.3 Results and discussion

5.3.1 XRD characterization results of ferric precipitates

The X-ray diffraction pattern and the corresponding elemental composition for the precipitates formed at different initial solution pH are shown in Figure 5.1 and Table 5.1 respectively. The XRD analyses in Figure 5.1 show that the precipitates synthesized in the pH range studied are almost identical with the exception of the precipitate formed at pH 1.9 and 2.2, which shows a few more peaks that did not appear at low pHs (See Figure C 1 on appendix C for illustration of extra peaks). The low background counts indicate that the precipitates are well crystalline. The results indicate that the most dominant mineral is K-jarosite with some trace amounts of H_3O^+ substitution, suggesting the possibility of a mixed mineral of potassium-hydronium jarosite. Such substitution is possible because of the low levels of monovalent cations (Gramp et al., 2008).

The significant decrease in K^+ concentrations with increase solution pH as evidential from Table 5.1, indicates that part of K^+ is possibly substituted by H_3O^+ in the formation process (Liu et al., 2007). Even though the reaction medium contained high concentrations of NH_4^{2+} (703.10mg/L) compared to K^+ (601.44 mg/L) the XRD results showed no traces of ammonia. This could be attributed to the fact that the formation of K-jarosite requires low concentrations of the monovalent cations (Nazari et al., 2014), as opposed to ammonium jarosite which requires much high levels of NH^+_4 (Gramp et al., 2008).

The presence of extra peaks on the precipitates formed at pH 1.9 and 2.2 indicates the presence of at least another phase. According to Bigham et al. (1996) and Bigham and Nordstrom (2000), jarosite dissolves at higher pHs to form goethite, or metastable phases, such as schwertmannite or ferrihydrite. Even though jarosite and schwertmannite coexist in situ and in vitro (Wang et al., 2006a), the extra peaks observed on the precipitates formed at pH 1.9 and 2.2 cannot be ascribed to schwertmannite. This is because one of the factors favouring schwertmannite formation, apart from high pH (Wang et al., 2006b), is extremely low concentrations of monovalent cations (Gramp et al., 2008) and the cationic concentrations in this study are quite significant.

To assign the extra peaks to possible phases, thermodynamic modeling (Visual MinteQ ver. 3.0) was conducted (Table 5.2). The simulation results showed the possible formation of ferrihydrite, goethite, hematite and lepidocrocite. The slight positive index for ferrihydrite and lepidocrocite indicate that, over a long period, ferrihydrite may precipitate at pH 2.2 and lepidocrocite at pH

1.9 and 2.2. The results also show high positive saturation index for hematite (1.909 – 7.007) over the pH range studied. However, the formation of this phase is not possible because of the low temperature employed in this study. According to Dutrizac (1990) and Kaksonen et al. (2014b), the conversion of jarosite to hematite is only possible at elevated temperatures. It should be noted that the utilized software is not based on recent thermodynamic data. For that reason, the extra peaks observed can, therefore, be ascribed to geothite. The formation of this phase is also supported by the well-crystalline appearance of the precipitate resulting from the low background counts (Rodger and Herbert, 1997).

The reported mol ratio of Fe/S for jarosite is 1.5 (Nurmi et al., 2010). The observed mol ratio of Fe/S (Table 5.1) in this study shows an indistinct relationship with increase initial pH. The high mol ratio obtained at pH 1.9 and 2.2 denotes the formation of other iron precipitates in addition to K-H_3O-jarosite, possibly the geothite that was detected by XRD patterns. The mol ratio for the precipitate formed at pH 1.7 was also higher than the theoretical mol ratio of 1.5 but because no extra peaks were detected by XRD patterns on this precipitate suggests this precipitate is likely to be poorly crystalline. The low mol ratio at pH 1.5 however, could be caused by the slowness and incompleteness formation of jarosite-type compounds at low pHs (Margulis et al., 1976), also noticeable from the low-intensity peaks (fig 5.1) and low saturation index (Table 5.2).

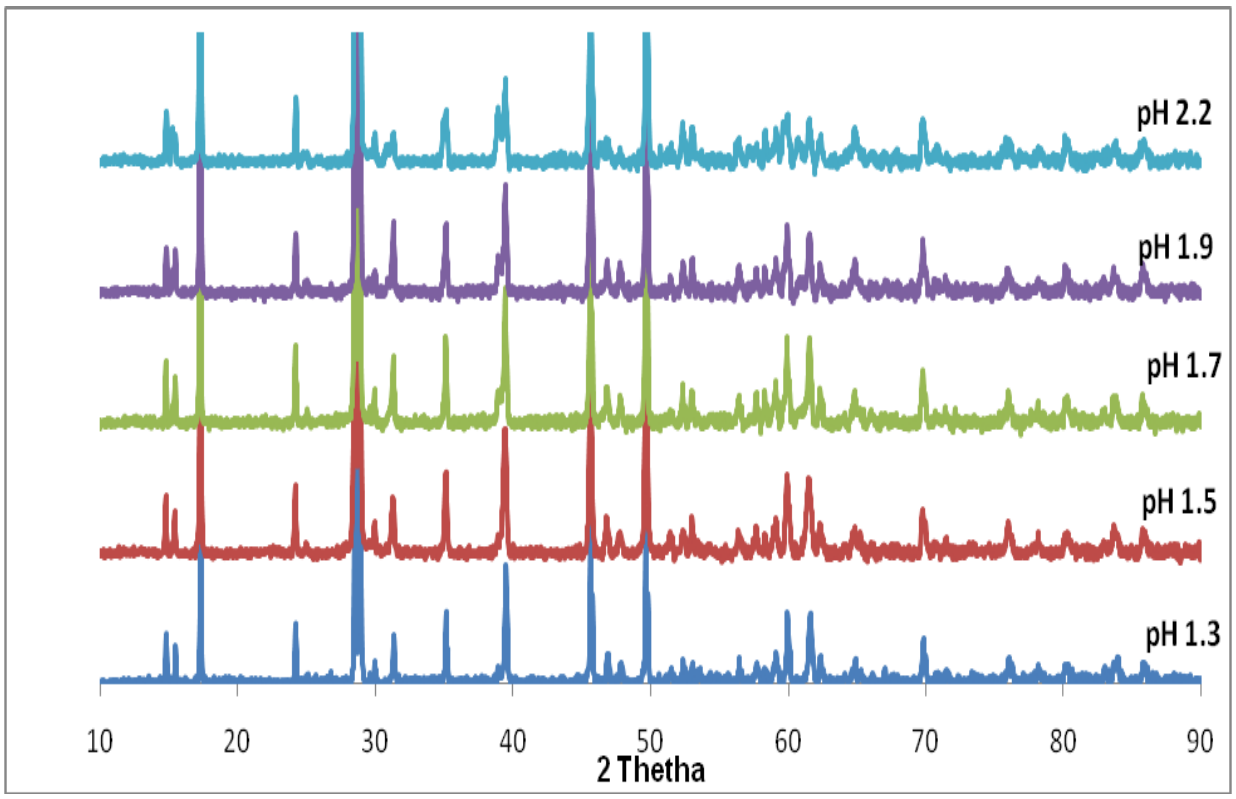

Figure5.1: XRD patterns of the ferric precipitates produced at different initial pH

Table 5.1: Elemental composition and molar ratio of the precipitates formed at different initial pH. Depending on the initial pH, the precipitates contained varying amounts of Fe (29.61 – 37.3%), K (1.4 – 5.26%) and S (11.11 – 13.61%) in (%w/w). The elemental composition of K decreased with increased in pH to values as low as 1.4.

	Element (weight %)			Molar ratio
pH	S	K	Fe	Fe:S
1.5	13.61	5.26	29.61	1.23
1.7	13.33	3.72	37.3	1.61
1.9	12.92	2.31	35.39	1.57
2.2	11.11	1.4	34.41	1.78

Table 5.2: The relationship between the pH and the saturation indexes of iron complex species in the biooxidation solution medium showing possible ferric ion precipitates at different initial pH, calculated using Visual Minteq

saturation index at different pH					
Mineral	1.3	1.5	1.7	1.9	2.2
Fe(OH)2 (am)	-11.907	-11.553	-11.192	-10.823	-10.258
Fe(OH)2 (c)	-11.828	-11.473	-11.113	-10.744	-10.179
Fe2(SO4)3(s)	-8.997	-8.839	-8.719	-8.632	-8.547
Fe3(OH)8(s)	-19.415	-17.95	-16.467	-14.963	-12.666
Ferrihydrite	-2.756	-2.202	-1.641	-1.072	-0.207
Ferrihydrite (aged)	-2.246	-1.692	-1.131	-0.562	0.303
Goethite	-0.27	0.285	0.846	1.414	2.28
Hematite	1.909	3.018	4.14	5.276	7.007
H-Jarosite	-2.966	-1.935	-0.92	0.085	1.584
K-Jarosite	1.273	2.496	3.705	4.906	6.699
Lepidocrocite	-1.494	-0.939	-0.379	0.19	1.055
Maghemite	-6.628	-5.519	-4.397	-3.261	-1.53
Melanterite	-1.492	-1.453	-1.426	-1.407	-1.39

*Oversaturation SI = (+), *Under saturation SI = (-)

5.3.2 Morphological appearance of ferric ion precipitates

Figure 5.2 shows the SEM images of the precipitates formed at different initial solution pHs. The morphologies of the precipitates in this study varied to some extent, but in general, the precipitates resembled potassium-jarosite. The particles appear as large aggregates of fairly unsmooth, coarse and rounded-like particles with surfaces covered by a crust of precipitate. This layer of crust was also observed by Grishin et al. (1988a) and its appearance denotes the presence of Hydronium jarosite (Bigham et al., 2010), which was also detected by XRD pattern. The crust formation on the particles became less with an increase in initial pH, promoting the formation of distinct particles. It can be concluded that, in general, changes in environmental pH play a vital role in the morphological variation of ferric ion precipitates.

The morphological results of the precipitates observed in this study are similar to the SEM images of ferric ion precipitates reported by Sasaki and Konno (2000). According to the work of these authors, the morphology of potassium-jarosite consists of round and granular particles with no sharp edges. The development, however, of sharp edges on the precipitates formed at

pH 1.9 and 2.2 is possibly attributed to the presence of the extra phase (goethite) detected by XRD patterns. The other contributing factor for the development of sharp edges could be the fact that the samples were held at desired initial pH for only 14 days, which might not have been sufficient for complete phase transformation (Bigham et al., 2010).

The morphologies of the precipitates presented in this study are different from the morphological structures reported by Gramp et al. (2008). This may be due to the difference in the type of strain used, time and conditions of crystallization. It is believed that the type of strain affects the crystallization rate of ferric ion precipitates (Sasaki and Konno, 2000) and the morphology thereof. Thus, it can be inferred that crystallization rate of ferric ion precipitates in media mediated by *Leptospirillum ferriphilum* is high, because of the unsmooth surfaces of precipitates, compared to media mediated by other microbes. This is because *Leptospirillum ferriphilum* are less sensitive to ferric ion (Rawlings et al., 1999) as opposed to other microbes.

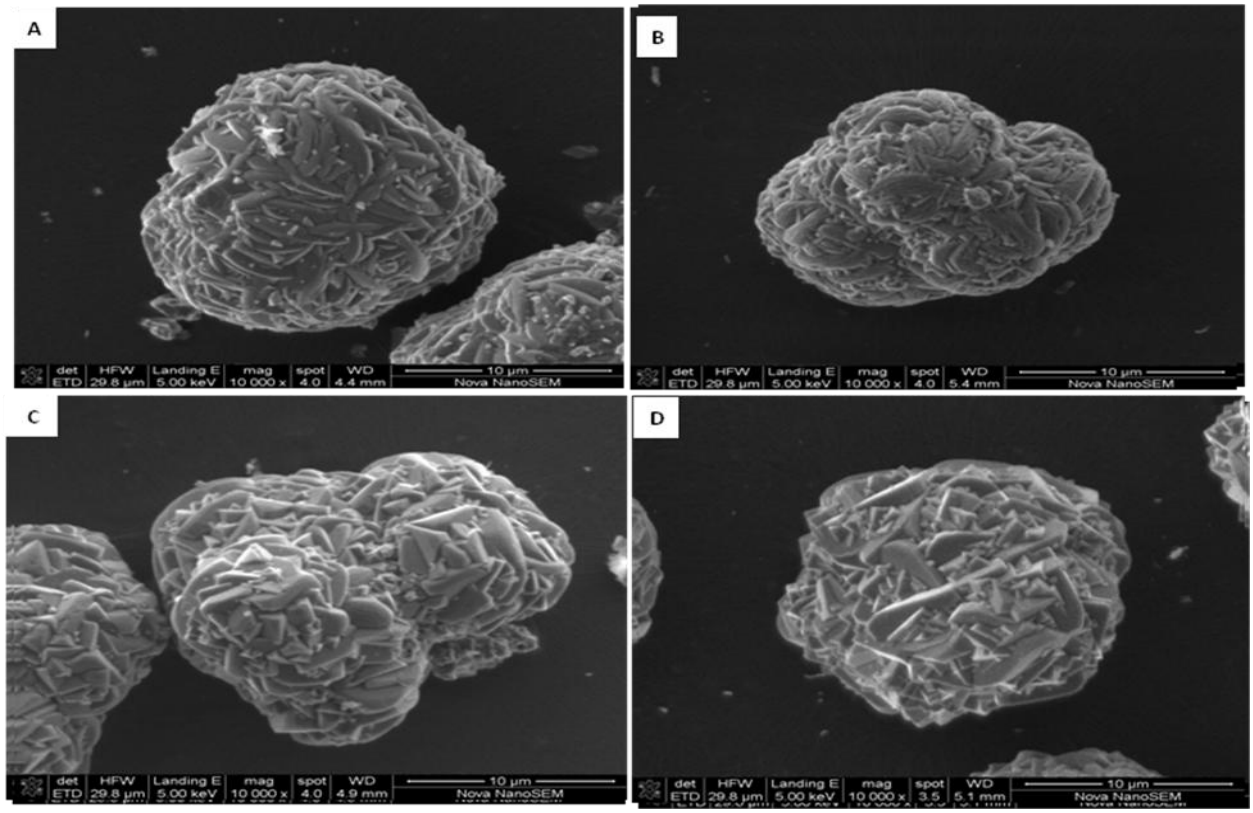

Figure 5.2: SEM analyses of ferric ion precipitates formed at different initial pH. A) 1.5, B) 1.7 C) 1.9 and D) 2.2

5.3.3 Particle Size distribution

The particle size distribution of particles formed after 5, 12 and 14 days is shown in Figure 5.3. These results were obtained in order to investigate whether there are primary species that serve as precursor for jarositic type compounds. The results show a monomodal distribution with peaks at 650, 890 and 350 nm after 5, 12 and 14 days respectively. The number of particles increased with increase in time interval, while the particle size increased then decreased due to high precipitation rates. The seemingly wide span distribution of particles supports the theory of the initial formation of monomer species which later develop into larger polymeric species by an aggregative mechanism (Flynn, 1984). These findings are in direct accord to the suggestions of Lazaroff et al. (1982) where the authors reported that jarosite-type compounds are unlikely to be the primary products of microbial oxidation and proposed the formation of polymeric intermediaries as precursors of jarosite-type compounds.

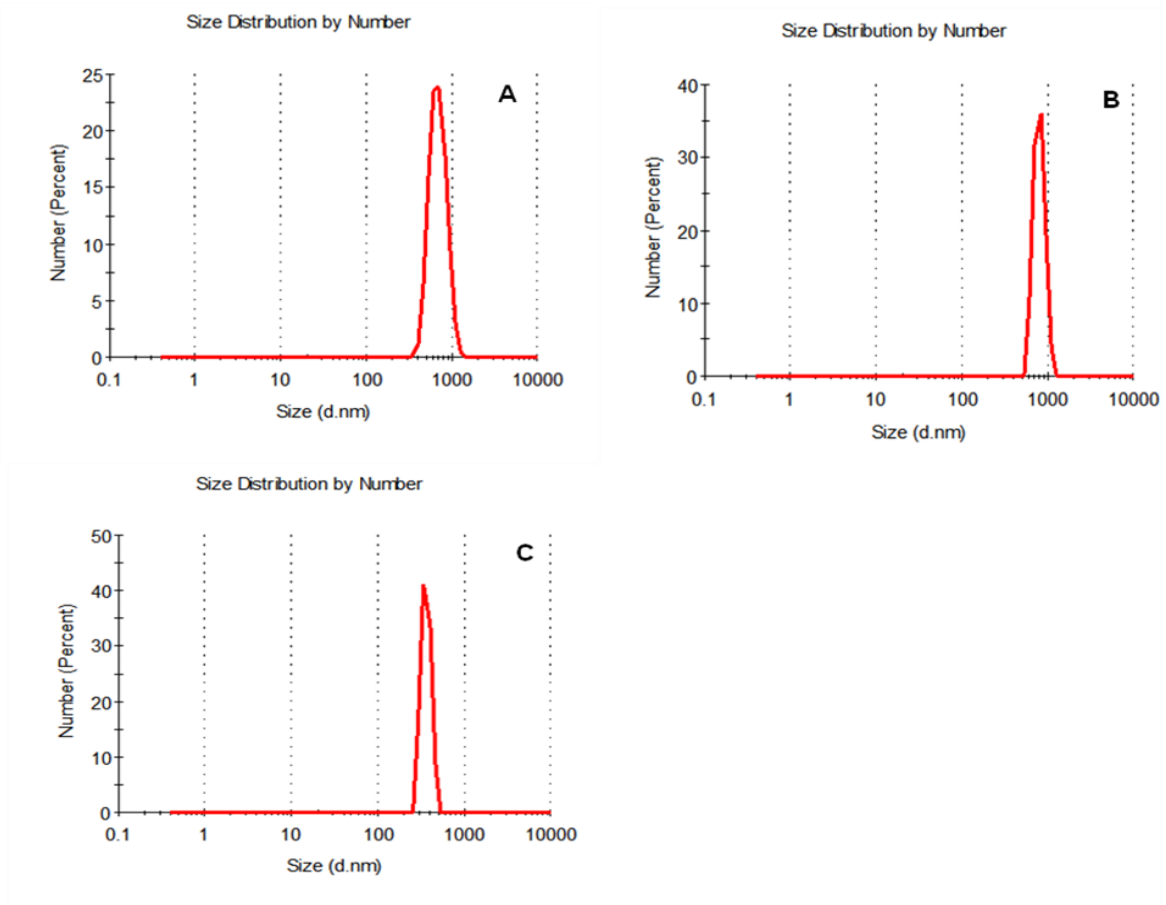

Figure 5.3: Evolution of precipitated particles with time at initial pH 1.5 after A) 5 days, B) 12 days and C) 14 days

The size distribution of the precipitated particles obtained at different initial pH is shown in Figure 5.4. The number distribution of the particles was narrower and monomodal with peaks at 250, 175, 101 and 25 nm for precipitates obtained at pH 1.5, 1.7, 1.9 and 2.2 respectively. The monomodal distribution of the particles corresponds to crystals of the same phase rather than crystals of different phases and for this reason the extra phases detected by XRD patterns on the precipitate formed at pH 1.9 and 2.2 could not be identified by PSD results, simply because this phase was not fully developed due to the incomplete phase transformation. The distribution of particles at high pH showed the formation of smaller particles while the precipitates formed at low pH had large particles. The smaller particles formed at high pH is attributed to rapid precipitation while the large particles formed at low pH is attributed to slow precipitation rate of ferric ion precipitates (Kaksonen et al., 2014b). Potassium jarosite is reported to have rapid precipitation rate at high pH (Nygjelten et al., 1999), this is consistent with the high amount of precipitate recovered at these pHs. The total number of particles increased with increase in initial pH due to the increase in the amount of precipitate formed. Approximately 41% of particles had a diameter of 250 nm and 50 % had a diameter of 118 nm for precipitates obtained at pH 1.5 and 2.2 respectively. Particle size distribution of ferric ion precipitates is affected by the rate of crystallization (Sasaki and Konno, 2000). The effect of crystallization is visible from SEM results in Figure 5.2. Crystallization became significant at pH > 1.7 as evidential by the development of sharp edges.

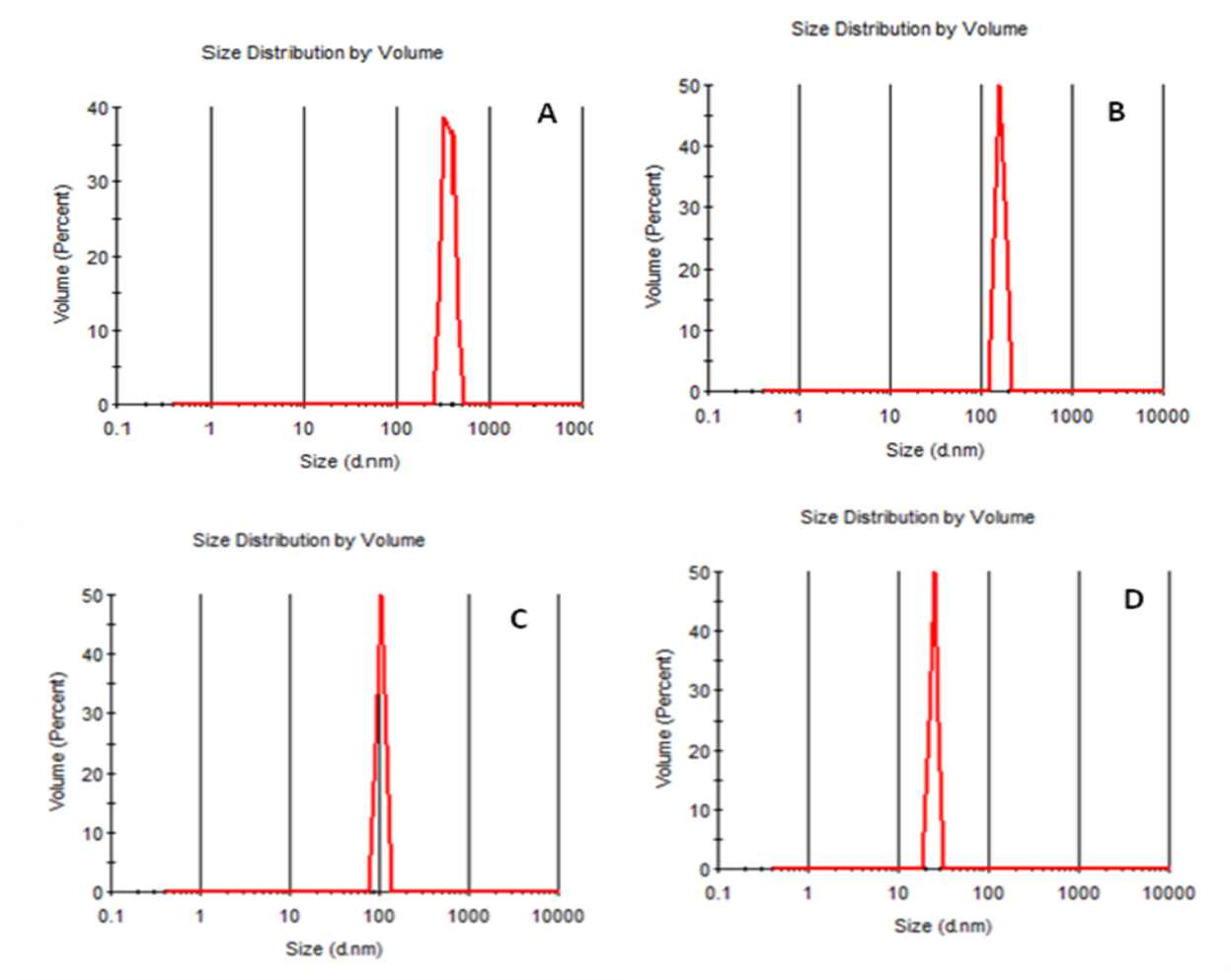

Figure 5.4: Particle Size Distribution of precipitates obtained at different initial pH A) 1.5, B) 1.7, C) 1.9 and D) 2.2

5.3.4 Surface charge of precipitates

The zeta potential-pH curve of ferric ion precipitates obtained at different initial pH values is shown in Figure 5.5 and was determined between pH ranges of 1.5 to 8. The maximum and minimum zeta potential measured was 9.1 and -.8.81 mV respectively which is within the general low-acceptable zeta potential values of +15 mV and -15mV (Ottewill, 1982). The precipitate obtained at pH 1.5 displayed a positive zeta potential over the pH range studied while the rest showed a different behavior. The iso-electric point (IEP) for the precipitates decreases with increase initial pH. Figure 5.5 indicates that the precipitates formed at pH 1.7 and 1.9 had IEP located at pH 2.8 and 2.25 respectively while the precipitate formed at initial pH

2.2 had two IEP located at pH 1.8 and 7.1 respectively. Sadowski et al. (2001) reported two iso-electric points (IEP) of pH 3.9 and pH 5.7 respectively for chemically synthesized jarosite. The difference in IEP between the precipitate formed in this study and the one synthesized by Sadowski et al. (2001) lies in the difference in method of preparation. The medium in which the precipitates in this study were synthesized contained a variety of anions and cations that could have attributed to the difference in IEP by adsorption onto the surface of the resulting precipitates. The second IEP at pH 7.1 for the precipitate formed at pH 2.2 is a result of the tendency of jarosite to ferric oxyhydroxides transfer (Sadowski et al., 2001), possibly the goethite detected by XRD patterns. The smaller IEP for the precipitates in this study is attributed to the attachment of microorganisms noticed by Chowdhury and Ojumu (2014) causing the surface of the precipitates to be partially covered by microbes thus bringing the IEP close to that of *Leptospirillum ferriphilum* which is located at pHs < 2 as reported by Gu et al. (2014).The decrease in IEP of the precipitates formed at higher pH from the IEP of 3.9 reported by Sadowski et al. (2001), is associated to the amount of precipitate formed at the respective pHs. Since the amount of precipitate was found to increase with increase initial pH, the decrease in IEP for precipitate formed at pH 2.2 was more pronounced due to the large amount of microorganisms attached.

Since the effective functional groups of ferric ion precipitates that contribute to the surface charge changes on precipitates have not been identified in literature, thermodynamic modeling (Visual MinteQ ver. 3.0) was conducted to assist in the interpretation of the zeta potential results. This was helpful in interpreting the possible adsorption of possible species onto surfaces of the precipitates. The simulation results showed the formation of different aqueous species (results not shown), but the concentration of SO_4^{-2} species was found to be very high and increased with increase in pH. The negative charge carried by the precipitates at pHs beyond their IEP could be attributed to the adsorption of SO_4^{2-} ions. The adsorption of SO_4^{2-} ions on iron precipitates was also reported by Jonsson (2003). The precipitate obtained at pH 2.2 showed a charge reversal at pH 6, a behavior that other precipitates did not reveal. This phenomenon could be due to the difference on the surface of this precipitate as a result of the presence of the extra phase that was detected by XRD pattern.

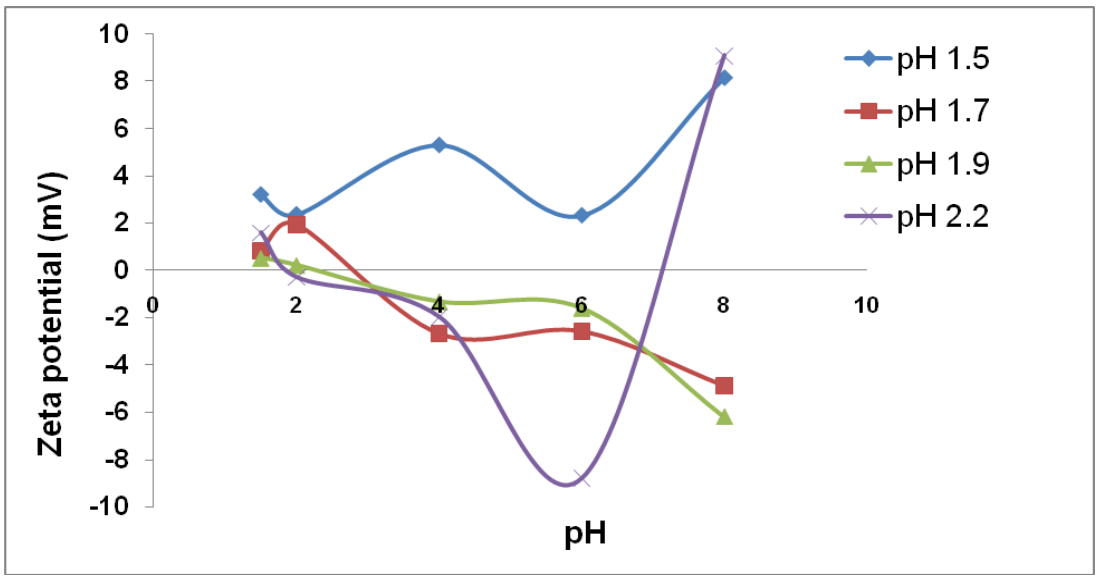

Figure 5.5: Zeta potentials vs pH of ferric ion precipitates obtained at different initial pH

The zeta potential vs pH curves of precipitates before and after adsorption is shown in Figure 5.6. For simplicity, the graphs are represented in different scales to accentuate the changes in zeta potential of each precipitate surface. From the curves, it is evident that the zeta potential for the precipitate formed at pH 1.5 did not change much after the adsorption experiments. This is because the precipitate surface was positively charged and therefore Cu^{2+} cannot adsorb onto the precipitate surface and cannot change the magnitude of the zeta potential. On the other hand, the zeta potential curves for other precipitates were different. In general, the zeta potential curves show that after adsorption experiments the zeta potential for each precipitate increased to positive values.

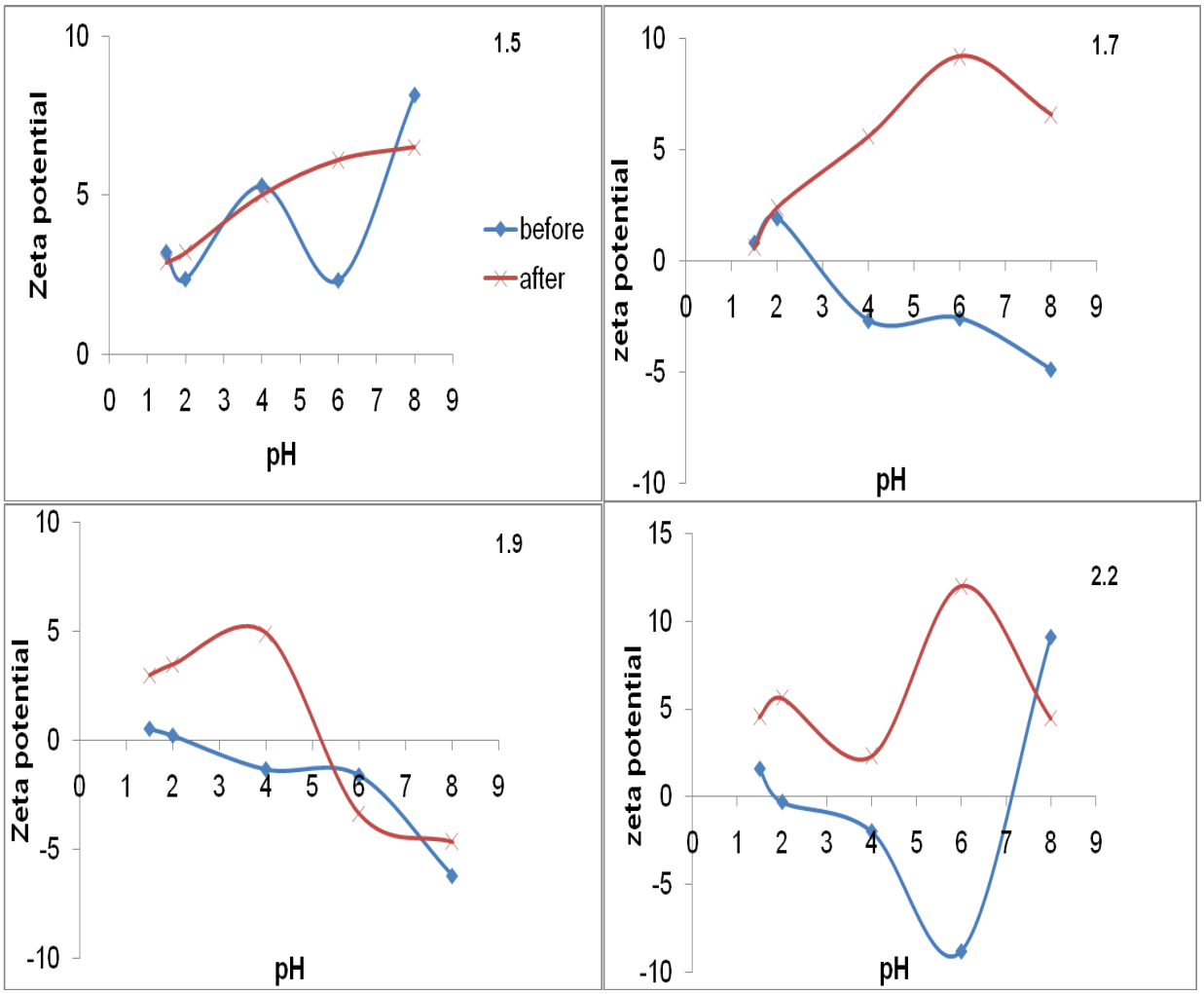

Figure 5.6: zeta potential of precipitates before and after adsorption experiments for different initial pH

For the purpose of this study and the prevailing conditions in biohydrometallurgy, it is important to restrict the interpretation of the zeta potential curves to pHs that are widely employed in biohydrometallurgy. Because of the low pH ranges of mostly studied microbes used in bioleaching (Ojumu, 2008) and the fact that jarosite dissolves at higher pH (Bigham et al., 1996), it is necessary to restrict the interpretation to experimental pH conditions. The results in Figure 5.6 were used to acquire the surface charge of precipitates at pHs correlating to the pHs of biooxidation experiments at which the precipitates were formed (Table 5.2).

Table 5.3 gives the surface charge of precipitates before and after adsorption. The general trend gathered from the Table is that the surface charge of ferric ion precipitates decreases with increase initial pH. Within the pH range studied, the precipitates formed at pH ≤ 1.9 were positively charged while the precipitate formed at pH 2.2 was negatively charged. From the results shown in Table 5.3 it follows that the magnitude of surface charge on precipitates obtained at different initial pH is consistent with the following order: precipitate at pH 2.2 < precipitate at pH 1.9 < precipitate at pH 1.7 < precipitate at pH 1.5. Because copper ions are positively charged, the electrostatic attraction forces between copper and the resulting precipitates are consistent with the following order: copper and precipitate formed at pH 1.5 < copper and precipitate formed at pH 1.7 < copper and precipitate formed at pH 1.9 < copper and precipitate formed at pH 2.2. The higher the electrostatic attraction between copper and the precipitate, the easier it will be for copper to adsorb onto the surface of the precipitate. Table 5.3 shows that the surface charge of precipitates formed at pH 1.9 and 2.2 increased considerably after adsorption experiments due to the large amount of copper adsorbed because of the weak electrostatic repulsion forces between the precipitate surface and copper ions. The adsorption of copper onto precipitates formed at lower pHs of 1.5 and 1.7 was insignificant because of the high electrostatic repulsion forces caused by the high positively charged surfaces of the precipitates. It should be kept in mind that the change in the surface charge of the precipitates is merely attributed to the adsorption of copper ions on the surface and not by the nature and concentration of the electrolyte since both are regarded insignificant to affect the surface charge (Marek, 2012).

The zeta potential results can also be used to infer the stability of the precipitates in solution where removal of undesired ferric ion precipitates is desired. Ferric ion precipitates are reported to interfere with process kinetics (Nurmi et al., 2010) and therefore its control and management in biohydrometallurgy is critical. Highly charged particles will repel each other and remain in solution while less charged particles will aggregate and settle down. The low surface charge on the precipitates indicated by the zeta potential results signifies that the precipitates formed in this study are stable due to the low electrostatic repulsion forces resulting from the low magnitude of surface charge promoting agglomeration and permitting easy removal from the process system. These results are in accordance with the findings of Kaksonen et al. (2014b).

Table 5.3: Surface charge of precipitates formed at different initial pH before and after adsorption experiments

pH	Surface charge before adsorption	Surface charge after adsorption
1.5	3.21	2.9
1.7	1.51	1.5
1.9	0.48	3.5
2.2	-0.5	5.25

5.4 Conclusion

This study was conducted to investigate the effect of initial pH on the surface properties of ferric ion precipitates formed during biooxidation of ferrous ion. This was to establish a relationship, if any, between initial pH and surface properties of precipitates. The resulting precipitates were characterized by XRD, SEM/EDS, PSD and zeta potential. The XRD patterns indicated that the formed precipitates in this study were potassium-hydronium jarosite with some phases of goethite on the precipitate formed at pH 1.9 and 2.2. The low background counts indicated that the precipitates were well crystalline and were free of amorphous phases. The SEM analyses showed the precipitates to possess smooth surfaces with no sharp edges, except for the precipitate formed at pH 1.9 and 2.2.

The PSD results showed that jarosite-type compounds do not form directly from solution but develop from polymeric intermediaries. The precipitates formed at high pH produced smaller particles due to the rapid rate of precipitation while larger particles were formed at low pH due to the slow precipitation rate. The number of particles was found to increase with an increase in pH due to increased amount of precipitate formed.

The zeta potential results showed that the precipitates formed at pH≤ 1.9 carried a positive charge while the precipitate formed at pH 2.2 carried a net negative charge. The IEP for the precipitates decreased with increase in pH decreasing electrostatic repulsion forces between the precipitate and copper ions. The magnitude of surface charge on precipitates was consistent with the following order: precipitate at pH 2.2 < precipitate at pH 1.9 < precipitate at pH 1.7 < precipitate at pH 1.5. Because the precipitate formed at pH 2.2 had less positive surface charge,

it scavenged more copper ions due to the weak electrostatic repulsion forces as opposed to the precipitate formed at pH 1.5.

The results show that the loss of valuable metals in biohydrometallurgy, due to adsorption on precipitates, is a result of the resulting surface charge of the precipitate. Highly positive charged precipitates showed less adsorption ability due to the high electrostatic repulsion forces while less positively charged precipitates showed higher adsorption ability due to the higher electrostatic attraction. In response to the recommendations drawn by Nheta and Makhatha (2013) of modifying precipitation process to reduce/prevent co-precipitation of base metals, the findings in this study show that in order to increase bioleach efficiency and prevent the loss of valuable metals, bioleach solution conditions should be maintained such that the resulting surface charge on the formed precipitate is highly positive.

Chapter 6

CONCLUSIONS AND RECOMMENDATIONS

6.1 Conclusions

The objective of this study was to investigate the surface properties of ferric ion precipitates formed during biooxidation of ferrous ion by *L. ferriphilum* in a CSTR and to quantify the resulting precipitates; with a view to provide an understanding of the effects of pH on the surface charge and the adsorption ability of the precipitates for valuable metals. Even though it is well understood that ferric ion precipitates interfere with process kinetics by decreasing the recovery of metals, no study has attempted to address this matter in detail. Moreover, studies on characterization of ferric ion precipitates only extend up to mineralogy, chemical composition and morphology and this information alone does not help understand the driving force for adsorption of metals. Hence, this study aims to narrow the gap by focusing on the surface properties of ferric ion precipitates with the hope that knowledge of the surface charge of precipitates will provide an indication on how valuable metals adsorb onto precipitates. Therefore, zeta potential measurements were conducted to investigate what role surface charge of precipitate play in the nature of adsorption of copper ions as well as what role initial pH play in modifying the precipitate surface charge. This knowledge will be useful in biohydrometallurgy such that it will help improve the recovery of valuable metals.

Although quantification studies have been extensively carried out, however, the majority of these studies were carried in shake flasks which do not simulate real bioleach operations, moreover, they were conducted for short durations. Hence, the reported values from these studies are not reliable for the following reasons: 1) the difference in hydrodynamics between shake flaks and real bioleach systems such as tanks etc. and 2) real bioleach systems can operate for durations as long as one year compared to 48h employed in some studies. These differences are what cause the difficulties encountered by scientists in upscaling lab work into industrial scale.

Quantification results showed that the amount of ferric ion precipitate formed increased from 4.31 to 13.36 g with an increase in initial pH (from 1.3 to 2.2). However, the amounts obtained in this study are quite high in comparison to literature values obtained at similar pHs. This is due to

the higher reactor volume and prolonged duration employed in this study as compared to other studies. The results revealed that significant precipitation of ferric ion occurred during the exponential phase. It was interesting to note that there was no significant precipitation during the stationary phase of the microorganism. This implies that precipitation of ferric ion is facilitated by the activity of the microorganisms.

Furthermore, the XRD patterns indicated that the formed precipitates in this study were potassium-hydronium jarosite with some phases of goethite on the precipitate formed at pH 2.2. The low background counts indicated that the precipitates were well crystalline and were free of amorphous phases. Also, the SEM analyses showed the precipitates to possess smooth surfaces with no sharp edges, except for the precipitate formed at pH 2.2. The PSD results showed that jarosite-type compounds do not form directly from solution but develop from polymeric intermediaries, supporting the proposition of Lazaroff et al. (1982). The number of particles was found to increase with an increase in pH due to increased amount of precipitate formed.

The zeta potential results showed that the precipitates carried a net positive charge over the experimental pH studied except for the precipitate formed at pH 2.2 which carried a slightly negative charge. The maximum and minimum zeta potential measured was +9.1 and -8.81 mV respectively. The IEP for precipitates decreased with increase in pH. The decrease in IEP of the precipitate formed at pH 2.2 was more pronounced due to the large number of microbes attached to the surface of the precipitate bringing the IEP close to the IEP of *L. ferriphilum.* The magnitude of the surface charge on precipitates was consistent with the following order: precipitate at pH 2.2 < precipitate at pH 1.9 < precipitate at pH 1.7 < precipitate at pH 1.5. Since the precipitate formed at pH 2.2 had less positive surface charge, it scavenged more copper ions due to the strong electrostatic attraction as opposed to the precipitate formed at pH 1.5.

The results show that the loss of copper was due to adsorption on precipitates is as a result of the surface charge of the precipitate. High positively charged precipitates showed less adsorption characteristics due to the high electrostatic repulsion forces as compared to less positively charged precipitates which promoted high electrostatic attraction forces. Therefore, it can be concluded that in order to increase bioleach efficiency and recovery of metals bioleach solution conditions should be maintained such that the resulting surface charge on the formed precipitate is more positive.

6.2 Recommendations for future studies

This study attempted to investigate the surface properties of ferric ion precipitates formed during biooxidation of ferrous ion at different initial pH to understand the driving force for the adsorption of valuable metals onto precipitates. The scope of this study did not cover the entire parameters that are encountered in bioleaching operations and that which are regarded to pose serious impacts on the adsorption of valuable metals onto ferric ion precipitates. For this reason, the following recommendations are suggested for future investigation.

- Ferric ion precipitation is inevitable in bioleaching processes. The only information that exists on ferric ion precipitation is the quantification. This only indicates the mechanistic relationship between operational conditions and the amount precipitated thereof. Hence, studies directed at investigating the kinetics of ferric ion precipitation in typical bioleach operational conditions are recommended to understand the kinetics rather than the quantity.

- During bioleaching of sulphide minerals, there is a constant generation of ferric ion accompanied by an increase in solution pH. Ferric ion become sparingly insoluble at higher pH that it tends to precipitate and results in the formation of different ferric ion precipitates. It is hypothesised that different types of ferric precipitates will have different surface properties resulting in different adsorption characteristics. Therefore, future work should be conducted to investigate the surface properties of the mostly found precipitates in bioleaching operations.

- This study was conducted at different initial pH while the temperature was kept constant at 35 ^{0}C. It is a well-known fact that biohydrometallurgy is depended on the activity of microbes which are temperature dependent. However, It is postulated that changes in temperature will not have major effects on surface charge of precipitates. Nonetheless, the adsorption tendencies of metals will be different. Further work should be carried out to investigate the effect of temperature on the adsorption of valuable metals onto ferric ion precipitates.

- This study was conducted to gain insight on the surface charge of ferric ion precipitates. The adsorption experiments carried out in this study were not extensive as the general idea was to establish a base case. Comprehensive work on the adsorption kinetics

needs to be carried out in order to obtain kinetic values for the adsorption of metals onto precipitates.

Chapter 7

REFERENCES

ACEVEDO, F. 2000. The use of reactors in biomining processes. *Electronic Journal of Biotechnology,* 3**,** 10-11.

ARCHER, K. H. 1997. *Potential of thermophilic bioleaching: effect of temperature on the process performance.* University of Cape Town.

BENNETT, J. & TRIBUTSCH, H. 1978. Bacterial leaching patterns on pyrite crystal surfaces. *Journal of Bacteriology,* 134**,** 310-317.

BIGHAM, J. M., JONES, F. S., ÖZKAYA, B., SAHINKAYA, E., PUHAKKA, J. A. & TUOVINEN, O. H. 2010. Characterization of jarosites produced by chemical synthesis over a temperature gradient from 2 to 40 °C. *International Journal of Mineral Processing,* 94**,** 121-128.

BIGHAM, J. M. & NORDSTROM, D. K. 2000. Iron and aluminum hydroxysulfates from acid sulfate waters. *Reviews in mineralogy and geochemistry,* 40.

BIGHAM, J. M., SCHWERTMANN, U., TRAINA, S. J., WINLAND, R. L. & WOLF, M. 1996. Schwertmannite and the chemical modeling of iron in acid sulfate waters. *Geochimica et Cosmochimica Acta,* 60**,** 2111-2121.

BOON, M. 1996. *Theoretical and experimental methods in the modelling of bio-oxidation kinetics of sulphide minerals*, TU Delft, Delft University of Technology.

BREED, A. & HANSFORD, G. 1999. Effect of pH on ferrous-iron oxidation kinetics of Leptospirillum ferrooxidans in continuous culture. *Biochemical engineering journal,* 3**,** 193-201.

BRIERLEY, C. 1997. Mining Biotechnology: Research to Commercial Development and Beyond. *In:* RAWLINGS, D. (ed.) *Biomining.* Springer Berlin Heidelberg.

BRIERLEY, C. L. 1982. Microbiological Mining. *Scientific America***,** 44-55.

BRIERLEY, C. L. 2008. How will biomining be applied in future? *Transactions of Nonferrous Metals Society of China,* 18**,** 1302-1310.

BRIERLEY, C. L. 2014. Bioleaching. In AccessScience. McGraw-Hill Education. http://dx.doi.org/10.1036/1097-8542.082525. Visited on 2015/07/23.

BRIERLEY, J. & BRIERLEY, C. 2001. Present and future commercial applications of biohydrometallurgy. *Hydrometallurgy,* 59**,** 233-239.

BRYNER, L. & ANDERSON, R. 1957. Microorganisms in Leaching Sulfide Minerals. *Industrial & Engineering Chemistry,* 49**,** 1721-1724.

BRYNER, L. C., BECK, J. V., DAVIS, D. B. & WILSON, D. G. 1954. Microorganisms in Leaching Sulfide Minerals. *Industrial & Engineering Chemistry,* 46**,** 2587-2592.

CASAS, J. M., LIENQUEO, M. E., CUBILLOS, F. & HERRERA, L. 2000. *MODELACION CINETICA DE LA PRECIPITACION DE HIERRO COMO JAROSITA EN SOLUCIONES LIXIVIANTES UTILIZANDO LA BACTERIA Thiobacillus ferroxidans.* Universidad de Santiago.

CASAS, J. M., VARGAS, T., MARTINEZ, J. & MORENO, L. 1998. Bioleaching model of a copper-sulfide ore bed in heap and dump configurations. *Metallurgical and Materials Transactions B,* 29**,** 899-909.

CHIRANJIT, M. 2013. *Characterization of argentojarosite synthesized withbiologically produced ferric sulfate solutions.* The Ohio State University.

CHOWDHURY, F. 2014. *The effects of temperature on the kinetics of microbial ferrous-iron oxidation in packed column bioreactor.* PhD thesis, Cape Peninsula University Of Technology, South Africa.

CHOWDHURY, F. & OJUMU, T. V. 2014. Investigation of ferrous-iron biooxidation kinetics by Leptospirillum ferriphilum in a novel packed-column bioreactor: Effects of temperature and jarosite accumulation. *Hydrometallurgy,* 141**,** 36-42.

CORAM, N. J. & RAWLINGS, D. E. 2002. Molecular relationship between two groups of the genus Leptospirillum and the finding that Leptospirillum ferriphilum sp. nov. dominates South African commercial biooxidation tanks that operate at 40 C. *Applied and Environmental Microbiology,* 68**,** 838-845.

CÓRDOBA, E., MUÑOZ, J., BLÁZQUEZ, M., GONZÁLEZ, F. & BALLESTER, A. 2008a. Leaching of chalcopyrite with ferric ion. Part II: Effect of redox potential. *Hydrometallurgy,* 93**,** 88-96.

CÓRDOBA, E. M., MUÑOZ, J. A., BLÁZQUEZ, M. L., GONZÁLEZ, F. & BALLESTER, A. 2008b. Leaching of chalcopyrite with ferric ion. Part I: General aspects. *Hydrometallurgy,* 93**,** 81-87.

CURUTCHET, G., POGLIANI, C., DONATI, E. & TEDESCO, P. 1992. Effect of iron (III) and its hydrolysis products (jarosites) onThiobacillus ferrooxidans growth and on bacterial leaching. *Biotechnology letters,* 14**,** 329-334.

DAOUD, J. & KARAMANEV, D. 2006. Formation of jarosite during Fe2+ oxidation by Acidithiobacillus ferrooxidans. *Minerals Engineering,* 19**,** 960-967.

DEVECI, H., AKCIL, A. & ALP, I. 2004. Bioleaching of complex zinc sulphides using mesophilic and thermophilic bacteria: comparative importance of pH and iron. *Hydrometallurgy,* 73**,** 293-303.

DEVISIA, P. & NATARAJA, K. A. 2004. Bacterial leaching. *Biotechnology in the mining industry*.

DREISINGER, D. 2006. Copper leaching from primary sulfides: Options for biological and chemical extraction of copper. *Hydrometallurgy,* 83**,** 10-20.

DUNCAN, D. W., LANDESMAN, J. & WALDEN, C. C. 1967. ROLE OF THIOBACILLUS FERROOXIDANS IN THE OXIDATION OF SULFIDE MINERALS. *Canadian Journal of Microbiology,* 13**,** 397-403.

DUTRIZAC, J. E. 1990. Converting jarosite residues into compact hematite products. *JOM***,** 36 - 39.

DUTRIZAC, J. E. 1999. The effectiveness of jarosite species for precipitating sodium jarosite. *JOM,* 51**,** 30 - 32.

DUTRIZAC, J. E. & JAMBOR, J. L. 2000. Jarosites and their application in hydrometallurgy. *Reviews in Mineralogy and Geochemistry,* 40**,** 405-452.

EHRLICH, H. L. 2001. Past, present and future of biohydrometallurgy. *Hydrometallurgy,* 59**,** 127-134.

FLYNN, C. M. J. 1984. Hydrolysis of inorganic iron(III) salts. *Chemical Reviews,* 84**,** 31 -41.

GAHAN, C. S., SRICHANDAN, H., KIM, D.-J. & AKCIL, A. 2012. Biohydrometallurgy and biomineral processing technology: a review on its past, present and future. *Research Journal of Recent Sciences ISSN,* 2277**,** 2502.

GASHAROVA, B., GOTTLICHER, J. & BECKER, U. 2005. Dissolution at the surface of jarosite: an in situ AFM study. *Chemical Geology,* 215**,** 499 - 516.

GRAMP, J. P., JONES, F. S., BIGHAM, J. M. & TUOVINEN, O. H. 2008. Monovalent cation concentrations determine the types of Fe (III) hydroxysulfate precipitates formed in bioleach solutions. *Hydrometallurgy,* 94**,** 29-33.

GRISHIN, S. I., BIGHAM, J. M. & TOUVINEN, O. H. 1988a. Characterization of Jarosite Formed upon Bacterial Oxidation of Ferrous Sulfate in a Packed-Bed Reactor. *Applied and environmental microbiology,* 54**,** 3101 - 3106.

GRISHIN, S. I., BIGHAM, J. M. & TUOVINEN, O. H. 1988b. Characterization of jarosite formed upon bacterial oxidation of ferrous sulfate in a packed-bed reactor. *Applied and environmental microbiology,* 54**,** 3101-3106.

GU, G.-H., HU, K.-T. & SHUANG-KE, L. 2014. Surface characterization of chalcopyrite interacting with *Leptospirillum ferriphilum Transactions of Nonferrous Metals Society of China,* 24**,** 1898 - 1904.

HUDSON-EDWARDS, K. A. & WRIGHT, K. 2011. Computer simulations of the interactions of the (012) and (001) surfaces of jarosite with Al, Cd, Cu^{2+} and Zn. *Geochimica et Cosmochimica Acta,* 75**,** 52 - 62.

JENSEN, A. B. & WEBB, C. 1995. Ferrous sulphate oxidation using thiobacillus ferrooxidans: a review. *Process Biochemistry,* 30**,** 225-236.

JIANG, H. & LAWSON, F. 2004. Reaction mechanism for the formation of ammonium jarosite: thermodynamic studies and experimental evidence. *Mineral processing and extractive metallurgy* 113**,** 175 - 181.

JIN, J., SHI, S.-Y., LIU, G.-L., ZHANG, Q.-H. & CONG, W. 2013. Comparison of Fe^{2+} oxidation by *Acidithiobacillus ferrooxidans* in rotating-drum and stirred-tank reactors. *Transactions of Nonferrous Metals Society of China,* 23**,** 804 - 811.

JONSSON, J. 2003. *Phase transformations and surface chemistry of secondary iron minerals formed from acid mine drainage.* PhD Thesis, Umea University.

JU, S., ZHANG, Y., XUE, P. & WANG, Y. 2011. Clean hydrometallurgical route to recover zinc, silver, lead, copper, cadmium and iron from hazardous jarosite residues produced during zinc hydrometallurgy. *Journal of Hazardous Materials,* 192**,** 554 - 558.

KAKSONEN, A. H., MORRIS, C., REA, S., LI, J., JASONWYLIE, USHER, K. M., GINIGE, M. P., CHENG, K. Y., HILARIO, F. & PLESSIS, C. A. D. 2014a. Biohydrometallurgical iron oxidation and precipitation: Part I—Effect of pH on process performance. *Hydrometallurgy,* 147-148**,** 255–263.

KAKSONEN, A. H., MORRIS, C., REA, S., LI, J., USHER, K. M., MCDONALD, R. G., HILARIO, F., HOSKEN, T., JACKSON, M. & DU PLESSIS, C. A. 2014b. Biohydrometallurgical iron oxidation and precipitation: Part II — Jarosite precipitate characterisation and acid recovery by conversion to hematite. *Hydrometallurgy,* 147–148**,** 264-272.

KAZADI, T. K. 2007. *Evaluation ofthe Redostat™ Device for the Study of Ferrous Iron Biological Oxidation Kinetics.* , University Of Cape Town.

LAZAROFF, N., SIGAL, W. & WASSERMAN, A. 1982. Iron oxidation and precipitation of ferric hydroxysulfates by resting Thiobacillus ferrooxidans cells. *Applied and Environmental Microbiology,* 43**,** 924-938.

LEDUC, L., TREVORS, J. & FERRONI, G. 1993. Thermal characterization of different isolates of Thiobacillus ferrooxidans. *FEMS microbiology letters,* 108**,** 189-193.

LIU, J.-Y., XIU, X.-X. & CAI, P. 2009. Study of formation of jarosite mediated by Thiobacillus ferrooxidans in 9K medium. *Procedia Earth and Planetary Science,* 1**,** 706-712.

LIU, J., LI, B., ZHONG, D., XIA, L. & QIU, G. 2007. Preparation of jarosite by Acidithiobacillus ferrooxidans oxidation. *Journal of Central South University of Technology,* 14**,** 623-628.

LIU, J., WEIJIN, W., ZHANG, X., MINGLONG, Z. & WENSONG, T. 2017. Adhesion properties of and factors influencing Leptospirillum ferriphilum in the biooxidation of refractory gold-bearing pyrite. *International Journal of Mineral Processing*.

LUNDGREN, D. G. & SILVER, M. 1980. Ore Leaching by Bacteria. *Annual Review of Microbiology,* 34**,** 263-283.

LUNG, T. N. 1986. The history of copper cementation on iron — The world's first hydrometallurgical process from medieval China. *Hydrometallurgy,* 17**,** 113-129.

MACDONALD, D. & CLARK, R. 1970. The oxidation of aqueous ferrous sulphate by Thiobacillus ferrooxidans. *The Canadian Journal of Chemical Engineering,* 48**,** 669-676.

MAREK, K. 2012. IEP as a parameter characterizing the pH-dependent surface charging of materials other than metal oxides. *Advances in Colloid and Interface Science* 171–172**,** 77–86.

MARGULIS, E., GETSKIN, L., ZAPUSKALOVA, N. & BEISEKEEVA, L. 1976. HYDROLYTIC PRECIPITATION OF IRON IN FE2 (SO4) 3-KOH-H2O SYSTEM. *ZHURNAL NEORGANICHESKOI KHIMII,* 21**,** 1818-1823.

MERUANE, G. & VARGAS, T. 2003. Bacterial oxidation of ferrous iron by Acidithiobacillus ferrooxidans in the pH range 2.5–7.0. *Hydrometallurgy,* 71**,** 149-158.

MHLANGA, S. S. 2011. *Investigating the relative adsorption of polymeric depressents of pure minerals.* MSc, University of Cape Town.

MOUSAVI, S., YAGHMAEI, S., SALIMI, F. & JAFARI, A. 2006. Influence of process variables on biooxidation of ferrous sulfate by an indigenous Acidithiobacillus ferrooxidans. Part I: Flask experiments. *Fuel,* 85**,** 2555-2560.

NAZARI, B., JORJANI, E., HANI, H., MANAFI, Z. & RIAHI, A. 2014. Formation of jarosite and its effect on important ions for Acidithiobacillus ferrooxidans bacteria. *Transactions of Nonferrous Metals Society of China,* 24**,** 1152-1160.

NEALE, J., GERICKE, M. & RAMCHARAN, K. 2011. THE APPLICATION OF BIOLEACHING TO BASE METAL SULFIDES IN SOUTHERN AFRICA: PROSPECTS AND OPPORTUNITIES. *The Southern African Institute of Mining and Metallurgy 6th Southern African Base Metals Conference* 367 - 388.

NEMATI, M., HARRISON, S., HANSFORD, G. & WEBB, C. 1998. Biological oxidation of ferrous sulphate by Thiobacillus ferrooxidans: a review on the kinetic aspects. *Biochemical engineering journal,* 1**,** 171-190.

NHETA, W. & MAKHATHA, M. E. Leaching of nickel from a jarosite precipitate with hydrochloric acid. 2013. International Conference on Chemical and Environmental Engineering (ICCEE'2013).

NURMI, P., ÖZKAYA, B., SASAKI, K., KAKSONEN, A. H., RIEKKOLA-VANHANEN, M., TUOVINEN, O. H. & PUHAKKA, J. A. 2010. Biooxidation and precipitation for iron and sulfate removal from heap bioleaching effluent streams. *Hydrometallurgy,* 101**,** 7-14.

NYAVOR, K., EGIEBOR, N. O. & FEDORAK, P. M. 1996. The effect of ferric ion on the rate of ferrous oxidation by *Thiobacillus ferrooxidans*. *Applied Microbiology and Biotechnology,* 45**,** 688 - 691.

NYGJELTEN, E., WÆRNES, O., THORSEN, G. & MÅLSNES, A. 1999. Particle morphology and filtration properties in alkali jarosite precipitation. *14th International Symposium on Industrial Crystallisation*.

OJUMU, T. V. 2008. *The effects of solution conditions on the kinetics of microbial ferrous-Iron oxidation by Leptospirillum ferriphilum in continuous culture.* PhD thesis, University of Cape Town.

OJUMU, T. V., HANSFORD, G. S. & PETERSEN, J. 2009. The kinetics of ferrous-iron oxidation by Leptospirillum ferriphilum in continuous culture: The effect of temperature. *Biochemical Engineering Journal,* 46**,** 161-168.

OJUMU, T. V. & PETERSEN, J. 2011. The kinetics of ferrous ion oxidation by Leptospirillum ferriphilum in continuous culture: The effect of pH. *Hydrometallurgy,* 106**,** 5-11.

OJUMU, T. V., PETERSEN, J. & HANSFORD, G. S. 2008. The effect of dissolved cations on microbial ferrous-iron oxidation by Leptospirillum ferriphilum in continuous culture. *Hydrometallurgy,* 94**,** 69-76.

OLSON, G., BRIERLEY, J. & BRIERLEY, C. 2003. Bioleaching review part B. *Applied microbiology and biotechnology,* 63**,** 249-257.

ONGENDANGENDA, H. & OJUMU, T. 2013. The effect of initial pH on the kinetics of ferrous-iron biooxidation at low temperature. *African Journal of Biotechnology,* 10**,** 1679-1683.

OTTEWILL, R. H. 1982. Concentrated dispersions. *Chemical Society Review Symposium Goodwin, J.W. (ed.). Royal Society of Colloidal Dispersions.***,** 197 - 217.

PETERSEN, J. & DIXON, D. G. 2006. Competitive bioleaching of pyrite and chalcopyrite. *Hydrometallurgy,* 83**,** 40-49.

PETERSEN, J. & DIXON, D. G. 2007. Modelling zinc heap bioleaching. *Hydrometallurgy,* 85**,** 127-143.

PHAM, A. N., ROSE, A. L., FEITZ, A. J. & WAITE, T. D. 2006. Kinetics of Fe(III) precipitation in aqueous solutions at pH 6.0–9.5 and 25°C. *Geochimica et Cosmochimica Acta,* 70**,** 640-650.

PINA, P. S., LEÃO, V. A., SILVA, C. A., DAMAN, D. & FRENAY, J. 2005. The effect of ferrous and ferric iron on sphalerite bioleaching with Acidithiobacillus sp. *Minerals Engineering,* 18**,** 549-551.

QIU, M., XIONG, S., ZHANG, W. & WANG, G. 2005. A comparison of bioleaching of chalcopyrite using pure culture or a mixed culture. *Minerals Engineering,* 18**,** 987-990.

RAWLINGS, D., TRIBUTSCH, H. & HANSFORD, G. 1999. Reasons why'Leptospirillum'-like species rather than Thiobacillus ferrooxidans are the dominant iron-oxidizing bacteria in many commercial processes for the biooxidation of pyrite and related ores. *MICROBIOLOGY-READING-,* 145**,** 5-13.

RAWLINGS, D. E. 2002. Heavy metal mining using microbes. *Annu Rev Microbiol,* 56**,** 65-91.

RAWLINGS, D. E. 2005. Characteristics and adaptability of iron-and sulfur-oxidizing microorganisms used for the recovery of metals from minerals and their concentrates. *Microbial cell factories,* 4**,** 13.

RAWLINGS, D. E., DEW, D. & DU PLESSIS, C. 2003. Biomineralization of metal-containing ores and concentrates. *Trends in Biotechnology,* 21**,** 38-44.

RODGER, B. & HERBERT, J. R. 1997. PROPERTIES OF GOETHITE AND JAROSITE PRECIPITATED FROM ACIDIC GROUNDWATER, DALARNA, SWEDEN. *Clays and Clay Minerals,* 45**,** 261 - 273

ROSSI, G. 1990. *Biohydrometallurgy.* McGraw - Hill, New York.

SADOWSKI, Z., POLOWCZYK, I., FARBISZEWSKA, T. & FARBISZEWSKA-KICZMA, J. 2001. Adhesion of jarosite particles to the mineral surface. 31**,** 95 - 103.

SASAKI, K. & KONNO, H. 2000. Morphology of jarosite-group compounds precipitated from biologically and chemically oxidized Fe ions. *The Canadian Mineralogist,* 38**,** 45-56.

SCHIPPERS, A., JOZSA, P. & SAND, W. 1996. Sulfur chemistry in bacterial leaching of pyrite. *Applied and Environmental Microbiology,* 62**,** 3424-31.

SCHIPPERS, A. & SAND, W. 1999. Bacterial Leaching of Metal Sulfides Proceeds by Two Indirect Mechanisms via Thiosulfate or via Polysulfides and Sulfur. *Applied and Environmental Microbiology,* 65**,** 319-321.

SILVERMAN, M. P. & EHRLICH, H. L. 1964. Microbial formation and degradation of minerals. *Adv. Appl. Microbiol,* 6**,** 153-206.

SMITH, J. R., LUTHY, R. G. & MIDDLETON, A. C. 1988. Microbial ferrous iron oxidation in acidic solution. *Journal (Water Pollution Control Federation)***,** 518-530.

SUZUKI, I. 2001. Microbial leaching of metals from sulfide minerals. *Biotechnology Advances,* 19**,** 119-132.

SVELHA, G. 1996. Vogel's qualitative inorganic analysis. Longman, Singapore.

TAO, H. & DONGWEI, L. 2014. Presentation on mechanisms and applications of chalcopyrite and pyrite bioleaching in biohydrometallurgy–a presentation. *Biotechnology Reports,* 4**,** 107-119.

TEKIN, D., YÖRÜK, S. & KOCADAGISTAN, E. 2013. Kinetics of Bacterial Reduction of Hematite by Acidithiobacillus ferrooxidans-r4A1FC2B3. *ASIAN JOURNAL OF CHEMISTRY,* 25**,** 8875-8878.

THIRD, K. A., CORD-RUWISCH, R. & WALTING, H. R. 2000. The role of iron-oxidizing bacteria in stimulation or inhibition of chalcopyrite bioleaching. *Hydrometallurgy,* 57**,** 225 - 233.

TORO, L., PAPONETTI, B. & CANTALINI, C. 1988. Precipitate formation in the oxidation of ferrous ions in the presence of Thiobacillus ferrooxidans. *Hydrometallurgy,* 20**,** 1-9.

VAN SCHERPENZEEL, D., BOON, M., RAS, C., HANSFORD, G. & HEIJNEN, J. 1998. Kinetics of ferrous iron oxidation by Leptospirillum bacteria in continuous cultures. *Biotechnology progress,* 14**,** 425-433.

VISHNIAC, W. & SANTER, M. 1957. THE THIOBACILLI. *Bacteriological Reviews,* 21**,** 195-213.

VOSSOUGHI, M., ALEMZADEH, I., ZARRABI, A., MOUSAVI, S. M. & YAGHMAEI, S. 2007. Copper Recovery from Chalcopyrite Concentrate by an Indigenous Acidithiobacillus ferrooxidans in Airlift Bioreactor. *Biophysics & Bioengineering***,** 91 - 97.

WANG, H., BIGHAM, J. M. & TUOVINEN, O. H. 2006a. Formation of schwertmannite and its transformation to jarosite in the.pdf. *Material Science and Engineering,* 26.

WANG, H., BIGHAM, J. M. & UOVINEN, O. H. 2006b. Formation of schwertmannite and its transformation to jarosite in the presence of acidophilic iron-oxidizing microorganisms. *Materials Science and Engineering: C,* 26**,** 588-592.

WANJIYA, M. 2013. *Investigation of bacterial ferrous iron oxidation kinetics in a novel packed-column reactor: pH and jarosite management.* Cape Peninsula University of Technology, South Africa.

WANJIYA, M., CHOWDHURY, F. & OJUMU, T. V. 2015. Solution Ph and Jarosite Management during Ferrous Ion Biooxidation in A Novel Packed-Column Bioreactor. *Advanced Materials Research,* 1130**,** 291 - 295.

WATLING, H. 2006. The bioleaching of sulphide minerals with emphasis on copper sulphides—a review. *Hydrometallurgy,* 84**,** 81-108.

WATLING, H. R., ELLIOT, A. D., MALEY, M., VAN BRONSWIJK, W. & HUNTER, C. 2009. Leaching of a low-grade, copper–nickel sulfide ore. 1. Key parameters impacting on Cu recovery during column bioleaching. *Hydrometallurgy,* 97**,** 204-212.

ZHU, L., LIN, C., WU, Y., LU, W., LIU, Y., MA, Y. & CHEN, A. 2008. Jarosite-related chemical processes and water ecotoxicity in simplified anaerobic microcosm wetlands. *Environmental geology,* 53**,** 1491-1502.

Chapter 8

APPENDIX A

Determination of concentrations of iron species

A1.1 Reagent preparation

A.1.1.1 Spekker acid

The spekker acid solution was prepared by mixing equal volumes of concentrated sulphuric acid (98% H_2SO_4) and phosphoric acid (85%) with water in a ratio of 3:4 (acid solution: distilled water).

- Measure 600 mL distilled water using a 2 L beaker
- Carefully add 225 mL of concentrated sulphuric acid (98%) and 225 mL of phosphoric acid (85%) by slowly pouring the acid mixture against the wall of the beaker (Caution: rapid addition of the acid mixture to the distilled water will result in heat of mixing which will cause localised boiling, especially when using concentrated H_2SO_4)
- Allow the mixture to cool to room temperature before transferring into a storage bottle.

A1.1.2 Ferric acid

The ferric acid solution was prepared from the spekker acid:

- Measure 600 mL distilled water using a 2 L beaker
- Slowly and carefully add 150 mL of spekker acid and then 300 mL of concentrated hydrochloric acid (32% HCl) to the distilled water.
- Agitate the mixture using a magnetic stirrer and allow to cool to room temperature before transferring into a storage bottle.

A.1.1.3 Stannous chloride solution ($SnCl_2$)

- Weigh out 30 g stannous chloride in a 200 mL beaker.
- Add 100 mL concentrated hydrochloric acid (32%) and agitate at 50°C until it dissolves completely.
- Allow to cool to room temperature and dilute with 200 mL distilled water

- Add a small amount of granular tin to the solution to retard precipitation

A.1.1.4 Mercuric Chloride solution ($HgCl_2$)

- Weigh out 50 g mercuric chloride in a 2 L beaker.
- Add 1 L of distilled water and agitate until the solute has dissolved completely (about 2 hours).
- Add a spatula tip of $HgCl_2$ and stir for 2 hours before storage

A.1.1.5 Potassium-hydronium Dichromate solution (0.0149 M $K_2Cr_2O_7$)

- Dry approximately 10 g of $K_2Cr_2O_7$ (Molar mass 294.20 g.mol-1) in an oven at 105 – 110°C for 1 – 2 hours. Cool in a desiccator.
- Accurately weigh out 8.78 g of the dried $K_2Cr_2O_7$ into a 100 mL beaker.
- Transfer quantitatively into a 2 L beaker.
- Add 1.5 L of distilled water and agitate until dissolved completely.
- Transfer quantitatively into a 2 L standard volumetric flask and fill to the 2 L mark with distilled water.

A.1.1.6 Barium Diphenylamine Sulphonate (BDS) solution ($C_{24}H_{20}BaN_2O_6S_2$)

- Weigh out 1.0 g of barium diphenylamine suphonate in a 250 mL beaker and add 100 mL of concentrated sulphuric acid (98%). Agitate until the solute has dissolved completely.

A1.2 Determination of ferrous ion concentration by titration with potassium-hydronium dichromate solution

- Pipette 5 mL of the required aliquot solution into a 125 mL conical flask.
- Add 10 mL of spekker acid solution.
- Add 2 – 3 drops of BDS indicator.

- Titrate the potassium-hydronium dichromate (0.0149 M $K_2Cr_2O_7$) solution until the first permanent
  colour change from yellow to intense purple is obtained.

- Ferrous ion concentration may be calculated using Equation A1.1:

$$Fe^{2+} = \frac{[K_2Cr_2O_7] \times V_T \times (55.84 \times 6)}{V_{solution}} \qquad \text{A.1.1}$$

Where:

$[Fe^{2+}]$ = Ferrous ion concentration (g.L-1)

$[K_2Cr_2O_7]$ = $K_2Cr_2O_7$ concentration (i.e. 0.0149 M $K_2Cr_2O_7$)

V_T = Titration volume (mL) (amount of 0.0149 M $K_2Cr_2O_7$ added)

$V_{Solution}$ = Solution aliquot volume (mL)

A1.3 Determination of total iron concentration by titration with potassium-hydronium dichromate solution

- Filter 5 mL aliquot of sample solution.
- Pipette the required amount of aliquot (i.e. 5 mL) into a 125 mL conical flask.
- Add 10 mL of spekker acid solution and heat until the mixture boils.
- Add stannous (SnCl2) solution dropwise until the yellow colour disappears completely.
- Add one extra drop and record the amount of stannous chloride added (Note: It is important to record this amount, especially when doing duplicate titrations since it gives some an idea of the amount of SnCl2 required for the next duplicate titrations).
- Allow the solution to cool to room temperature and add 10 mL of mercuric chloride (HgCl2) solution. A silky-white precipitate should appear. If no precipitate forms, too little

stannous chloride was added in step 4. If the precipitate is heavy and grey/black, too much stannous chloride was added. In either case, abort the experiment and start over.

- Add 3 – 4 drops of barium diphenylamine indicator solution (BDS) and titrate with the potassium-hydronium dichromate solution until the first permanent colour change from yellow to intense purple is obtained.

Total iron concentration may be calculated using Equation A1.2.

$$Fe^{T} = \frac{[K_2Cr_2O_7] \times V_T \times (55.84 \times 6)}{V_{solution}} \quad \text{A1.2}$$

Where:

$[Fe^T]$ = Total iron concentration (g.L-1)

$K_2Cr_2O_7$= $K_2Cr_2O_7$ concentration (i.e. 0.0149 M $K_2Cr_2O_7$)

V_T = Titration volume (mL) (amount of 0.0149 M $K_2Cr_2O_7$ added)

$V_{Solution}$ = Solution aliquot volume (mL)

A.1.4 Vishniac Trace Metal Solution

Vishniac Trace Metal Solution was prepared according to the method suggested by V and Santer (1957).

Weigh the reagents accurately and dilute to 1 L volume with distilled water (dH2O).

- Prepare 6% potassium-hydronium hydroxide (KOH) by weighing 15 g KOH and dilute to 250 mL with dH_2O.
- Dissolve 50 g EDTA (Ethylene diamine tetra acetic acid disodium salt dihydrate) in 200 mL of 6% KOH using a magnetic stirrer.
- In a separate 500 mL beaker weigh the salts listed below and dissolve in 400 mL dH_2O for 30 minutes using a magnetic stirrer.

$ZnSO_4.7H_2O$	22g
$CaCl_2.2H_2O$	9.24 g
$MnCl_2.4H_2O$	5.06 g
$FeSO_4.7H_2O$	5 g
$(NH_4)_6Mo_7O_{24}.4H_2O$	1.1 g
$CuSO_4.5H_2O$	1.58 g
$CoCl_2.6H_2O$	1.62 g

- Transfer the solution prepared in step 2 quantitatively into the solution prepared in step 3 and make up to 1 L with dH_2O by rinsing the 500 mL beaker with 400 mL dH_2O. A deep greenish brown solution should result.

APPENDIX B

B1 Zeta potential experimental Procedure:

A detailed procedure used for the zeta potential determination is shown below (Mhlanga, 2011):

- Weigh 0.375 g of precipitate into 500 cm^3 beaker
- Add 300 cm^3 10^{-3} M of $NaNO_3$ solution
- Stir well and split into 5 beakers (60 cm^3)
- Adjust pH to 1.5, 2, 4, 6, and 8 with H_2SO_4 and NaOH
- Condition for 30 minutes on a magnetic stirrer ensuring that the pH remains constant
- Pipette about 1 cm^3 of precipitate dispersion into a folded capillary, ensuring that there are no bubbles in the cell
- Place cell in the Zeta Sizer Nano Series to measure the electrophoretic mobility

B2 Raw data for zeta potential pH curves

B2.1 Zeta potential of precipitates before adsorption

Precipitate formed at pH 1.5

pH	Zeta potential Runs (mV)			
	Run 1	Run 2	Run 3	Average
1.5	0.482	0.58	0.543	0.535
2	0.251	0.191	0.233	0.225
4	-1.451	-1.52	-0.989	-1.32
6	-1.581	-1.68	-1.539	-1.6
8	-5.9	-6.5	-6.2	-6.2

Precipitate formed at pH 1.7

	Zeta potential runs (mV)			
pH	Run 1	Run 2	Run 3	Average
1.5	0.824	0.58	0.63	0.678
2	1.93	1.87	1.93	1.91
4	-2.68	-2.32	-2.47	-2.49
6	-2.58	-2.53	-2.72	-2.61
8	-4.88	-4.82	-5.3	-5

Precipitate formed at pH 1.9

	Zeta potential Runs (mV)			
pH	Run 1	Run 2	Run 3	Average
1.5	1.7	1.3	1.8	1.6
2	-0.936	-1.28	1.34	-0.292
4	-2.38	-1.81	-1.72	-1.97
6	-8.97	-8.75	-8.71	-8.81
8	9.2	8.8	9.3	9.1

Precipitate formed at pH 2.2

pH	Zeta potential Runs (mV)			
	Run 1	Run 2	Run 3	Average
1.5	0.482	0.58	0.543	0.535
2	0.251	0.191	0.233	0.225
4	-1.451	-1.52	-0.989	-1.32
6	-1.581	-1.68	-1.539	-1.6
8	-5.9	-6.5	-6.2	-6.2

APPENDIX C

C1 XRD diffractograms

Comparison of the diffractograms of the precipitate obtained at pH 2.2 with that obtained at pH 1.3 to show the extra peaks at pH 2.2.

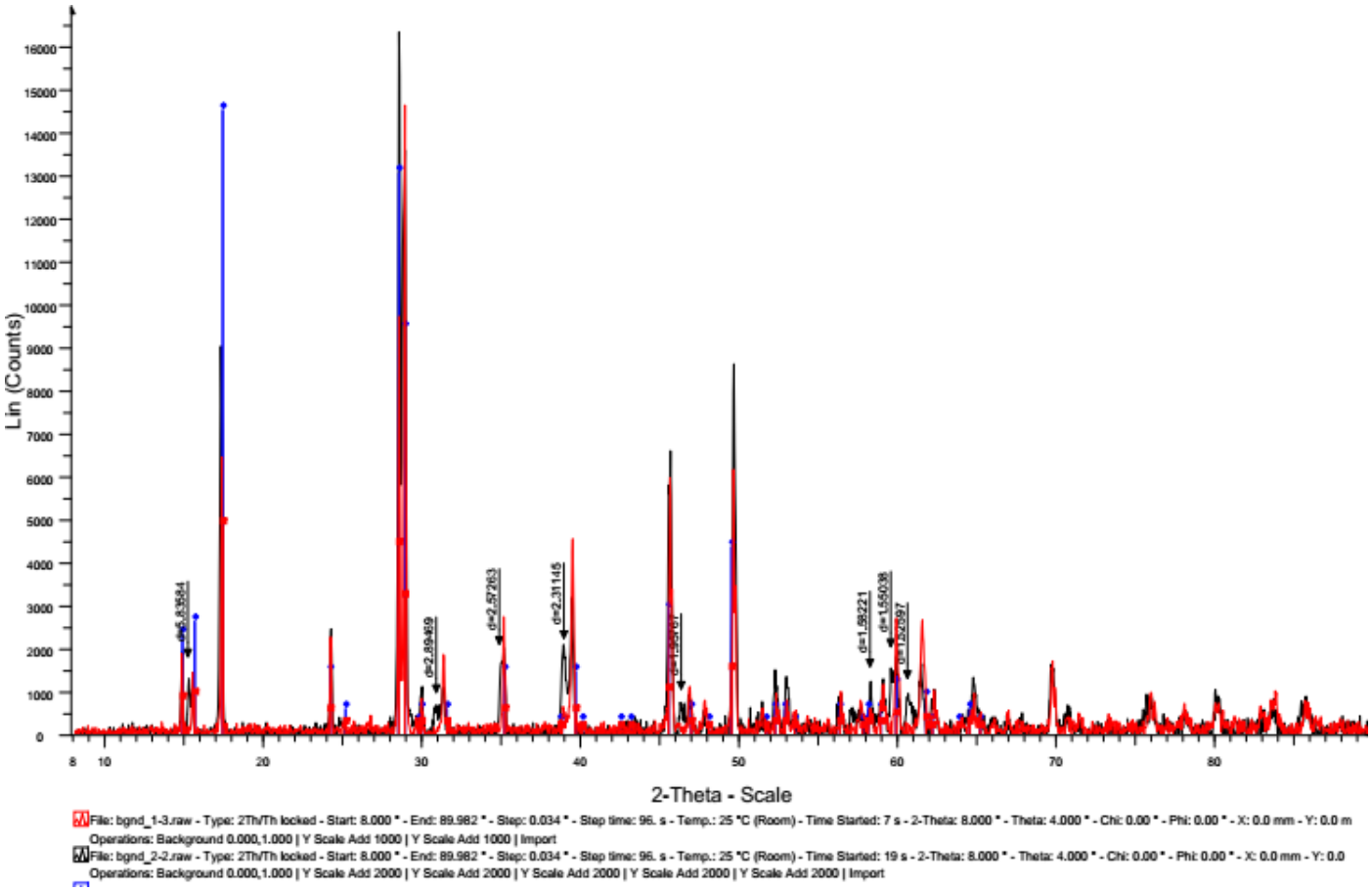

Figure C 1: Comparison of the diffractograms of the precipitate obtained at pH 2.2 with that obtained at pH 1.3 to show the extra peaks at pH 2.2

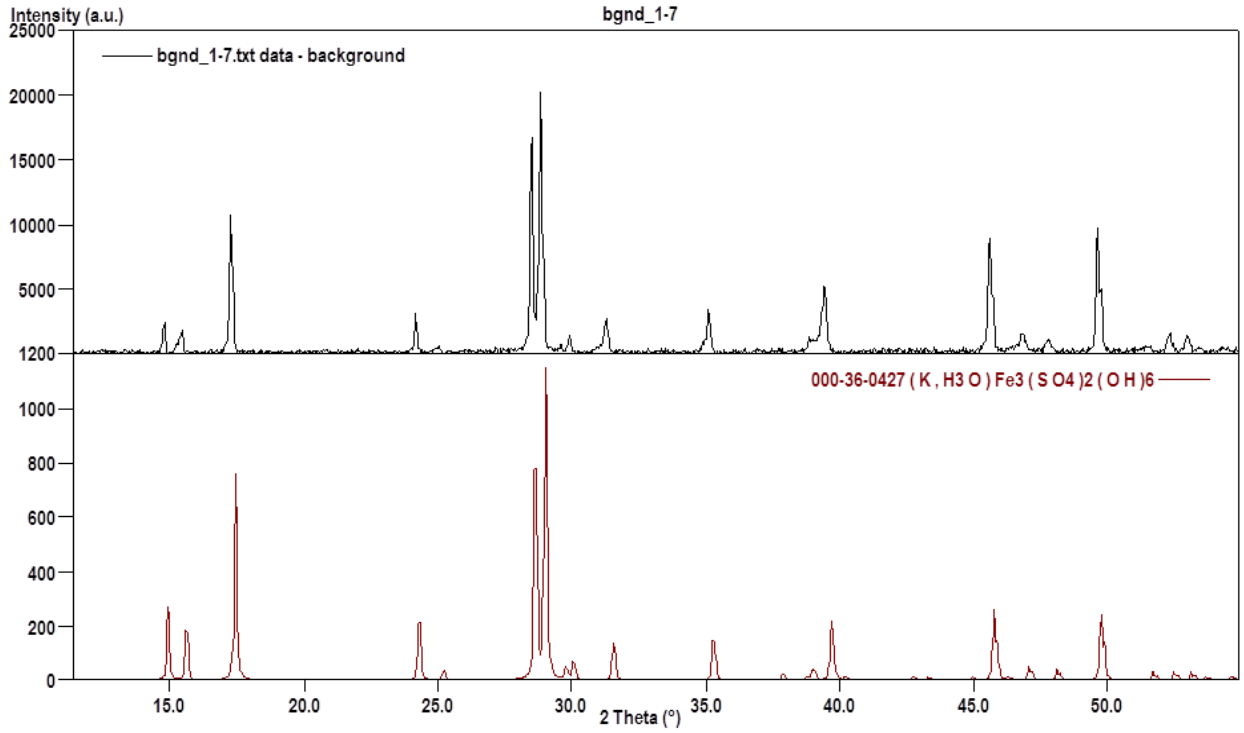
Intensity (a.u.)
bgnd_1-7
bgnd_1-7.txt data - background
000-36-0427 (K , H3 O) Fe3 (S O4)2 (O H)6
2 Theta (°)

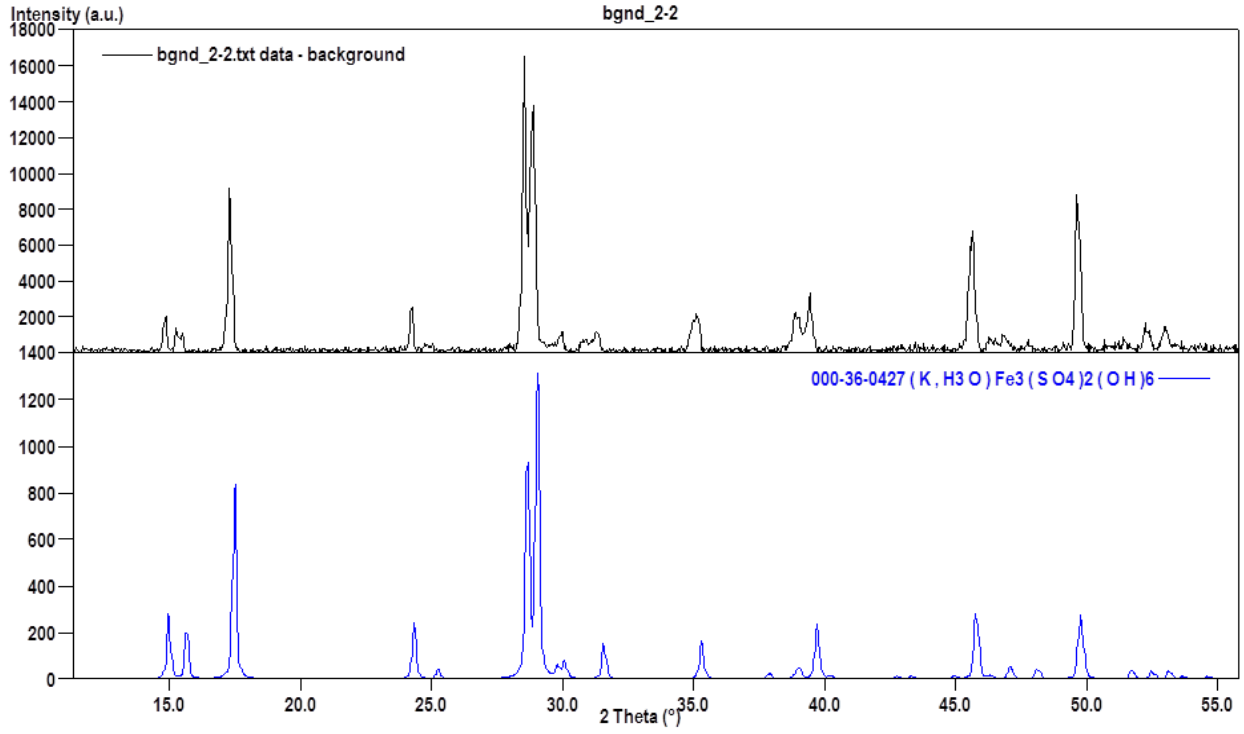
Intensity (a.u.)
bgnd_2-2
bgnd_2-2.txt data - background
000-36-0427 (K , H3 O) Fe3 (S O4)2 (O H)6
2 Theta (°)